CONTROLS ON FAULT-ZONE ARCHITECTURE AND FLUID FLOW IN POORLY CONSOLIDATED SEDIMENTS: THE SAND HILL FAULT, CENTRAL NEW MEXICO

Michiel R. Heynekamp

Submitted in Partial Fulfillment
of the Requirements for the Degree of
Master of Science in Geology

Earth and Environmental Science
New Mexico Tech
Socorro, NM 87801
May 3, 1998

Abstract

Faults in poorly consolidated sediment and their influence on fluid flow are poorly understood, despite the fact that many of the aquifers in the southwestern U.S. and hydrocarbon reservoirs in the world are situated in basins filled with poorly consolidated sediment and cut by numerous faults. In order to better understand how such faults influence fluid flow, determination of the controls on fault-zone architecture is useful. In this study I have characterized a fault that cuts poorly consolidated sediment in order to determine these controls. The Sand Hill fault, Albuquerque Basin, central New Mexico, was selected because it is exceptionally well exposed and cuts a variety of poorly consolidated sediments.

The architecture of the Sand Hill fault zone varies in a qualitatively predictable manner. The grain size and bed thickness of sediments adjacent to the Sand Hill fault controlled whether deformation was distributed or localized within the fault zone, and what the contribution of each bed was to the fault zone. Where the adjacent sediments are thickly bedded and >~18% sand, and clay beds are thin and rare, the fault zone is wide and structurally complex. Where the adjacent sediments are thick and $\geq$~ 18% clay and silt, or thin clay-rich beds interspersed with sub-equal numbers of thin sand-rich beds, the zone is narrow and structurally simple.

The fault zone is preferentially cemented with respect to adjacent sediments. Cemented zones are found nearly everywhere in the hanging wall (eastern or basinward side) of the fault that the hanging wall sediments are sands and gravels. The cemented zones are commonly flanked by elongate concretions

that are believed to record the orientation of groundwater flow at the time of their formation. The elongate concretions indicate that fluid flow was dominantly sub-vertical and parallel to the fault zone. Previous work has indicated that flow in surrounding sediments went from NW to SE, toward the fault. The cements are best developed where both the hanging wall and footwall sediments are coarse-grained. These relationships imply that at the time of cement formation there was both cross-fault and fault-parallel flow.

Acknowledgments

I wish to thank the New Mexico Bureau of Mines and Mineral Resources for their financial support of my project. Without their support, this thesis would not have been possible. Furthermore I would like to thank Exxon's EPR division, the USGS EDMAP program, and the New Mexico Tech Graduate Office for their financial support. I am indebted to my parents' financial support of my undergraduate degree; without their assistance in gaining a solid foundation I would not have been able to pursue this research.

I would like to personally thank Laurel Goodwin for all of the time she has devoted to this project and me. Not only has she been an excellent advisor in coursework, research direction, and general guidance, but she has been the best writing instructor, editor, and professor I have had the honor to work for. I also would like to thank Peter Mozley for his guidance and direction in this project. I also need to thank him for introducing me to the pleasures of field work when I worked for him as an undergraduate which is one of the primary reasons I had the interest to pursue and enjoy my time in the field at the Sand Hill fault. Bill Haneberg has provided the need for this study by making it applicable to future and ongoing studies. I would like to thank him for his interest in this work and all of his very helpful suggestions. Kurt Vollbrecht volunteered advice throughout this project and I owe much of my success to him. Kurt taught me how to approach many of the problems encountered along the way [during this project] and provided me with the motivation needed to overcome the difficulties encountered during the course of this project. Chris Dimeo was a great help on this project in the field and in many discussions.

On a final and most important note, I wish to thank Molley McFadden for being as patient and loving as she has been over the past six years. She has been supportive of my work and has been a great help in maintaining my emotional and physical well being. Thanks for being there.

Table of Contents

Plates

Figures

Tables

Introduction:

Faults can act as either conduits or barriers to subsurface fluid flow, with permeability characteristics that may vary over time (e.g. Knipe, 1993, 1997). A fault's influence on fluid flow depends greatly on the type and distribution of adjacent lithologies, deformational structures and fabrics, and the effects of diagenesis within the fault zone (Knipe, 1993; Gibson, 1994). Understanding the distribution of these features is essential in determining where, and if, a fault zone will act as a seal, a window, or both with respect to fluid flow. Faults can cut a variety of materials ranging from crystalline to sedimentary rock to unconsolidated sediment. The structures formed in a fault zone and their influence on flow are largely dependent on the type of rock or sediment faulted. The effects of fault-zone deformation and diagenesis, and their influence on fluid flow have been studied in sedimentary rocks (Pittman, 1981; Knipe, 1993; Gibson, 1994; Antonellini and Aydin, 1994, 1995), but not poorly consolidated sediments. This thesis is focused on the characteristics of a fault in poorly consolidated sediments.

The influence that a fault will have on fluid flow depends in large part on fault-zone architecture. Fault-zone architecture is the spatial arrangement and character of distinct structural elements. The architecture of a fault zone is dependent on many factors including the mechanical behavior of adjacent lithologies, the magnitude of displacement, the crustal level at which faulting takes place, and the faulting history (Caine et al., 1996). The spatial arrangement and hydraulic properties of the different fault-zone units determine how a fault influences fluid flow. Before the effects of faulting on fluid flow in poorly

consolidated sediment can be evaluated, the controls on fault-zone architecture and permeability structure for these faults must be known.

Many of the world's large groundwater aquifers and hydrocarbon reservoirs are situated in basins filled with poorly consolidated sediments and dissected by numerous faults (e.g., Anderson et al., 1988; Mifflin, 1988). An understanding of how these faults behave mechanically and their influence on fluid flow will help to better evaluate and use our groundwater and petroleum resources and understand contaminant transport within these basins. The first step in evaluating the influence of a fault on fluid flow is to characterize the fault-zone structures and diagenetic features.

I investigated controls on fault-zone architecture in poorly consolidated sediments using a combination of detailed mapping and grain-size analysis of fault-zone units and adjacent sediments. The Sand Hill fault, central New Mexico, was selected for this study because of its excellent exposure, created through a combination of preferential cementation of the fault zone and badlands erosion. I have determined that the grain size and clay content of sediments juxtaposed by the fault in part control the architecture of the Sand Hill fault zone. The vertical spacing between and thickness of clay-rich beds adjacent to the fault also appears to be controlling whether the fault zone will be wide and structurally complex or narrow and structurally simple. It is possible to constrain the influence that the fault may have had on past groundwater flow by examining the distribution of fault-zone cements, assuming that the degree and amount of cementation are a proxy for flux magnitude (Mozley and Davis, 1996). It is also possible to infer the direction of paleoflow by examining the

orientations of concretions developed within and outside the fault zone (Mozley and Goodwin, 1995; Mozley and Davis, 1996).

The Sand Hill fault is similar to the many other normal faults throughout the Basin and Range province that cut poorly consolidated sediments and have displacements of tens of meters or more. Many of these faults are not well exposed, making it difficult to determine their architecture. The controls of adjacent sediment type on fault-zone architecture discussed herein may be used to qualitatively predict the architecture of poorly exposed faults where sufficient data on adjacent sediment types are available.

Previous work

Fault-zone architecture and terminology

Fault zones can be divided into distinct structural units. These fault-zone units are defined on the basis of macroscopic structures, which have hydrologic significance. When these units are integrated with permeability data, a conceptual model of fault-related fluid flow can be constructed (e.g. Caine et al., 1996).

Previous workers have divided fault zones into a centrally located gouge or core zone and bounding damage zones (Sibson, 1977; Aydin, 1978; Chester and Logan, 1986; Smith et al., 1990; Byerlee, 1993; Gibson, 1994; Caine et al., 1996). The core zone is the structural, lithologic, and morphologically distinct portion of a fault zone where most of the displacement is accommodated. It may contain single slip surfaces (Caine et al., 1996), unconsolidated clay-rich gouge (Anderson et al., 1983), brecciated and geochemically altered areas (Sibson, 1977), and cataclasite zones (Chester and Logan, 1986). The damage zone consists of

the subsidiary structures that bound the fault core and may contain minor faults, veins, fractures, cleavage, and folds (Caine et al., 1996).

Caine et al. (1996) outlined a fault-zone model based on the different fault-zone architectural elements to help understand the permeability structure of a fault. There are three elements in their basic model: 1) a core zone, 2) bounding damage zones, and 3) undeformed protolith or country rock. Different fluid flow properties are assigned to each element in the model. The core has the lowest permeability due to grain-size reduction and possible mineral precipitation, the damage zone has the highest permeability due to the network of subsidiary structures, and the protolith has a mid-range permeability and porosity that have neither been enhanced nor reduced by faulting.

In Caine et al.'s (1996) model, the volume percentage of core zone and damage zone present determines a fault's influence on fluid flow. The core essentially acts as a barrier and the damage zone as a conduit. Both architectural elements need not be present, which results in four end member possibilities: 1) no core and wide damage zone: a distributed conduit; 2) a well developed core with wide damage zone: a combined conduit-barrier; 3) a well developed core with no damage zone: a localized barrier; or 4) both a poorly developed core and damage zone: a localized conduit. It is important to realize that fault-zone architecture may change with time and that the properties of the damage or core zones may change as well (i.e. diagenesis may result in filling of open fractures; Knipe, 1993).

This model can be used to evaluate how a fault might influence fluid flow if the variations in fault-zone properties, such as width of architectural elements, density of subsidiary structures, core-zone clay content, presence of a core zone,

and degree of mineralization can be determined. Many of these properties are believed to be dependent on the mechanical behavior of the intact protolith, which can control whether deformation is localized or distributed where the fault zone cuts different units (Caine et al., 1996).

The localization or distribution of deformation is important because it determines the fault-zone architecture and which of the four possibilities in Caine et al.'s model will exist. Localization of deformation results in a fault zone with a narrow or absent damage zone, but with a well developed core zone. Distribution of deformation results in a wider fault zone with a well developed damage zone, although the core may be absent.

In order to develop accurate, quantitative fluid flow models for faults in poorly consolidated sediment, a conceptual model of fault zones in poorly consolidated sediments is required. For the conceptual model to be useful, the architectural elements must be identified based upon their hydraulic characteristics and ability to be easily identified in the field. The various architectural elements of the fault zone should be based upon macroscopic structures that have hydraulic significance. Structural features, including slip surfaces, foliations, and deformation bands, have been shown to modify the original porosity and permeability of sedimentary rocks (Pittman, 1981; Jameson and Stearns, 1982; Underhill and Woodcock, 1987; Antonellini and Aydin, 1994; Fowles and Burley, 1994; Antonellini and Aydin, 1995). Faults in poorly consolidated sediments can also reduce permeability up to three orders of magnitude (Sigda et al., 1996), and have been inferred to result in a fault-parallel permeability anisotropy (Goodwin and Haneberg, 1996). By defining fault-zone

units, the influence of fault zones in poorly consolidated sediment on fluid flow can be addressed.

Sand Hill fault

The Sand Hill fault zone is located along the western margin of the Albuquerque basin (Fig. 1). It is one of the major normal faults bounding the Rio Grande Rift and strikes roughly north-south for approximately 50 km (Kelley, 1977). The fault separates syn-rift units of the late Oligocene to middle Miocene lower Santa Fe Group from the Pliocene-Pleistocene upper Santa Fe Group (Hawley and Haase, 1992; Hawley et al., 1995; Fig. 2). The Santa Fe Group comprises sediments filling the Rio Grande rift and ranges in thickness from 1,000 m along the basin margins to 5,000 m in the central basin area (Fig. 2; Hawley et al., 1995).

The Sand Hill fault is a growth fault that has experienced a history of episodic movement as first inferred by Wright (1946). Displacement of the base of the Santa Fe Group is ~600 m and varies little from south of the study area to north of the study area (Hawley et al., 1995; Hawley, pers. comm., 1997). My work indicates that the uppermost unit of the Santa Fe Group is locally displaced ~10 m.

The Sand Hill fault is preferentially cemented with calcite, causing it to locally stand above the adjacent sediments like a wall. Mozley and Goodwin (1995) described the fault-zone cements, including oriented concretions or flow features that are commonly present. The orientation of these concretions is interpreted to represent the orientation of groundwater flow at the time of their

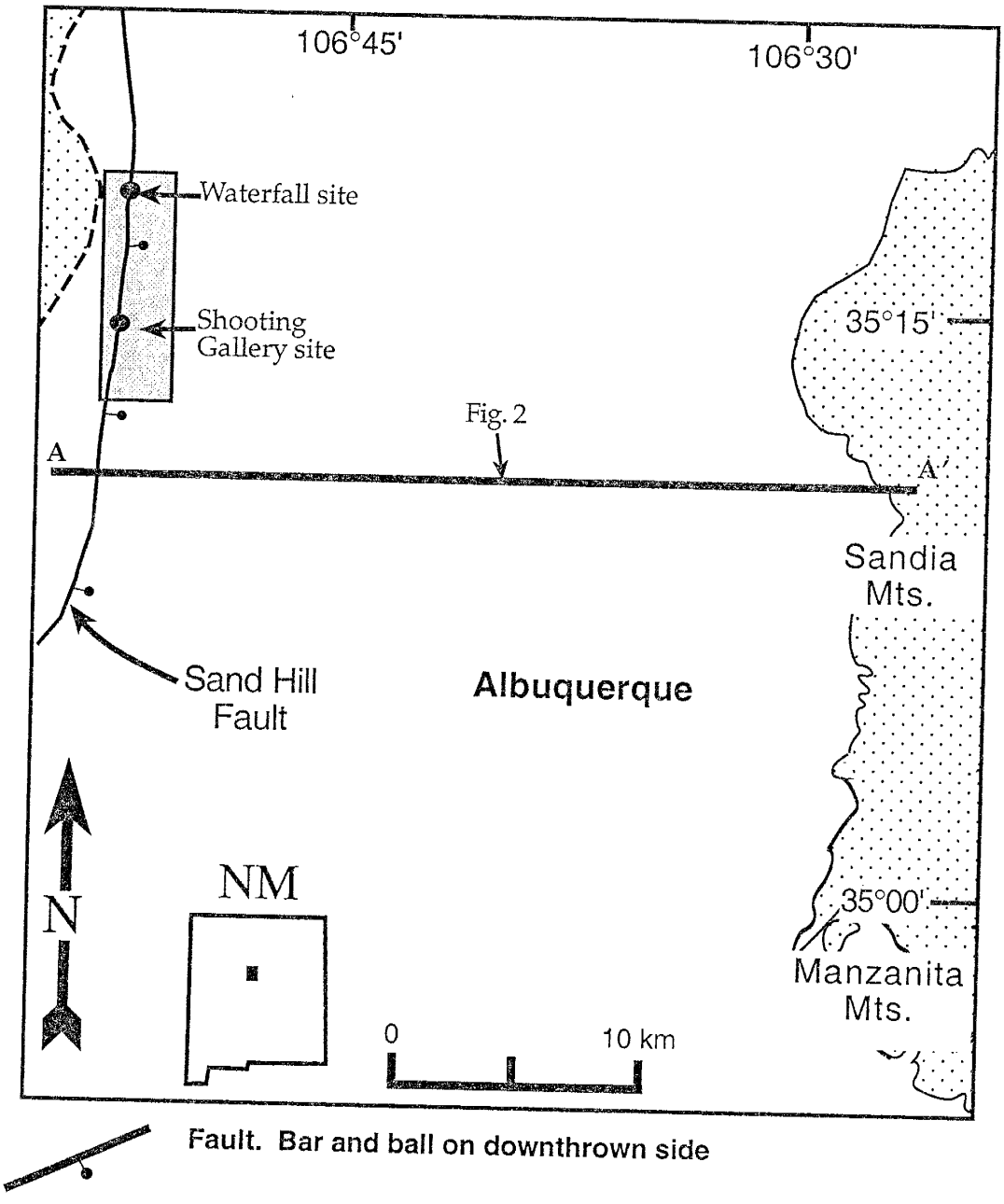

Figure 1. Map of Albuquerque Basin, central New Mexico, showing Sand Hill fault zone, pre-rift units, detailed study sites, and location of Fig. 2 cross section. Box shows extent of 1:6,000 map. Modified after Hawley et al. (1995).

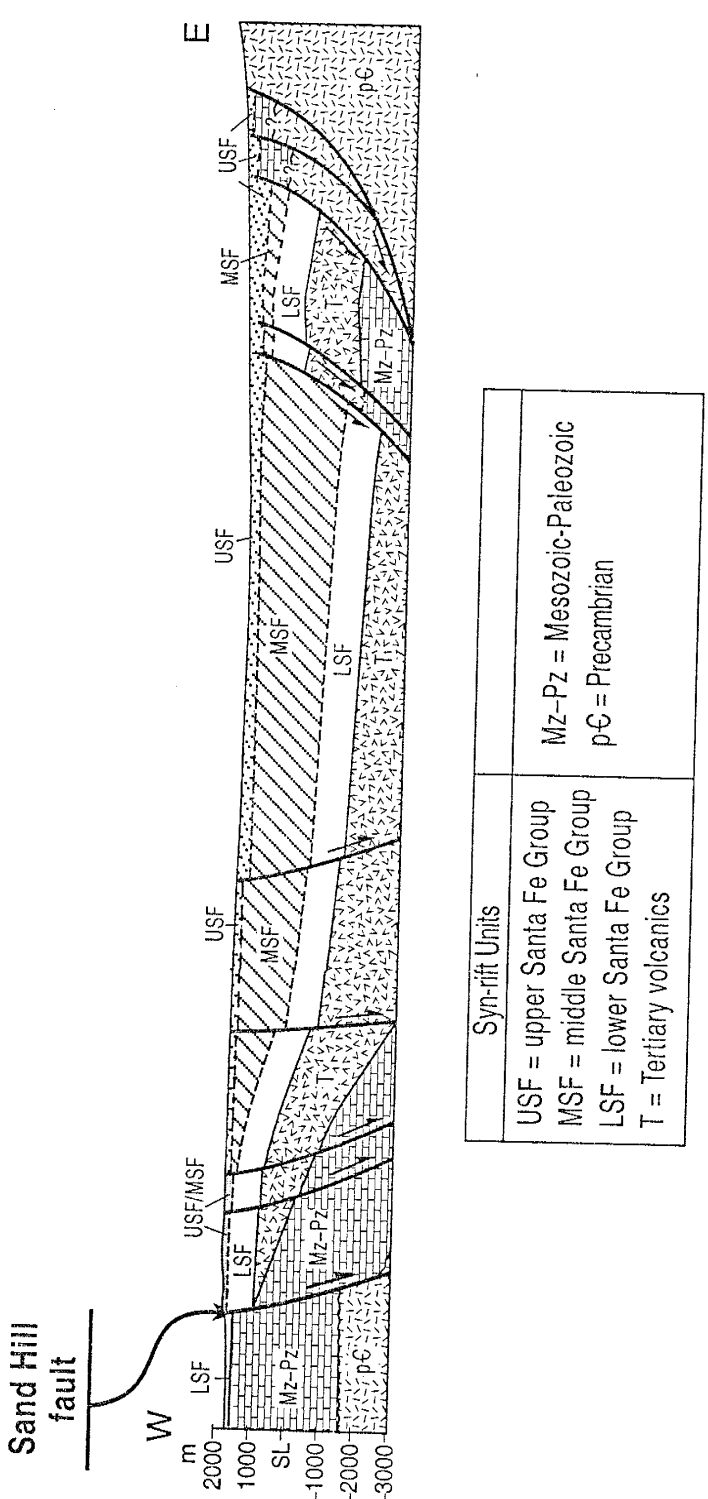

Figure 2. Cross illustrating major faults and lithologic units of the Albuquerque Basin, Rio Grande Rift. Location of the Sand Hill fault is indicated. After Hawley et al. (1995)

formation and may give insight into syn-diagenetic fault-zone permeabilities and flow conditions.

Stratigraphy

The Santa Fe Group consists of syn-rift basin-fill deposits including fluvial, eolian, and lacustrine sediments. It is divided into two unconformity-bounded formations within the study area: the Zia formation of the lower Santa Fe Group, (Fig. 2) and the overlying Sierra Ladrones formation of the upper Santa Fe Group, (Fig. 2; Tedford, 1982; Cather et al., 1997).

The Zia Formation consists of eolian, tributary axial-fluvial, and local playa deposits. The eolian system is dominated by a sandstone lithofacies. The tributary axial-fluvial system is divided into two lithofacies within the study area according to Cather's (1997) criteria: a sandstone-mudstone and a sandstone lithofacies (Cather et al., 1997). The Zia formation is estimated to be a maximum of 200 m thick although it is not fully exposed within the study area.

The Sierra Ladrones Formation (Machette, 1978) consists of tributary axial-fluvial deposits. The unit is divided into four textural lithofacies including conglomerate, conglomerate-sandstone, sandstone, and sandstone-mudstone, and has a maximum exposed thickness of 50 m in the study area (Cather et al., 1997). The section of the fault selected for this study borders the western edges of the Sky Village SE and Volcano Ranch 7.5′ quadrangles, approximately 30 km northwest of Albuquerque, New Mexico (Fig 1).

Field Studies of the Sand Hill fault zone and Adjacent Areas

Mapping Strategy

Reconnaissance mapping was performed at 1:24,000 to determine the continuity of the fault zone, the location of any major splays or other large structural features, and to select representative areas for detailed study. The resulting map was incorporated into the Sky Village SE 7 1/2' quadrangle map of Cather et al. (1997). More detailed mapping was done at 1:6,000 (Plate 1) to evaluate variations in displacement and cementation along strike and to determine if a relationship between age of sediments and fault-zone characteristics existed. This mapping was performed using air photogrammetry and traditional field mapping methods. Map units were determined according to Cather's (1997) classification, which designates units according to age, formation, depositional system, and textural lithofacies (Table 1).

Table 1. Classification of map units following Cather (1997)

Unit name	Age of Unit	Unit Formation	Depositional System	Textural Lithofacies
QTsacs	Quaternary-Tertiary	Sierra Ladrones	Axial-fluvial	conglomerate-sandstone
QTsasm	Quaternary-Tertiary	Sierra Ladrones	Axial-fluvial	sandstone-mudstone
QTsas	Quaternary-Tertiary	Sierra Ladrones	Axial-fluvial	sandstone
Tzasm	Tertiary	Zia	Axial-fluvial	sandstone-mudstone
Tzam	Tertiary	Zia	Axial-fluvial	mudstone
Tzas	Tertiary	Zia	Axial-fluvial	sandstone
Tzes	Tertiary	Zia	Eolian	sandstone
Tzsm	Tertiary	Zia	Axial-fluvial	silty mudstone

Characteristics of the sediments cut by the Sand Hill fault

The Zia formation (lower Santa Fe Group) is only exposed in the footwall of the Sand Hill fault. The beds and units of the Zia formation are continuous

throughout the map area and can be correlated from north to south. Zia sediments in the southern part of the map area are dominantly fluvial with mostly thin (1-3 m thick) sand and clay beds. Zia sediments adjacent to the fault in the northern part of the map area are dominantly thickly bedded (10-15 m scale; Beckner, 1996), well-sorted eolian sands with rare thin clay beds.

The Sierra Ladrones formation (upper Santa Fe Group) can be divided into three units bound by unconformities adjacent to the Sand Hill fault. Both the lower and middle units are found only in the hanging wall whereas the upper unit has been deposited across the fault in the Red Hill vicinity (Plate 1).

QTsas (Table 1), the oldest unit exposed in the hanging wall, has an outcrop thickness of 35-40 m but may be significantly thicker because the lower contact isn't exposed in the study area. The unit is characterized by 3-5 m thick uncemented sand beds that typically fine upwards from thin basal gravels and locally contains 1-5 cm thick clay drapes at bedding surfaces. Trough cross bedding, scour-and-fill structures, and imbrication features are common.

QTsasm (Table 1), is approximately 5-10 m thick and coarsens from the south to the north according to my mapping. To the south, thinly bedded, poorly cemented to uncemented muds and silts with minor sands characterize QTsasm. To the north, QTsasm is characterized by thickly bedded, fine- to very coarse-grained sands and gravels displaying trough crossbedding and horizontal stratification; locally QTsasm may be bioturbated, destroying original sedimentary features. QTsasm therefore displays the greatest variation in grain size of the three units, ranging from very clay-rich sediments to sands and gravels with little clay.

Uncemented coarse gravels and sands characterize the uppermost unit, QTsacs. A coarse gravel of this unit, approximately 2-5 m thick, is deposited across and offset approximately 10 m by the Sand Hill fault in an area extending from Red Hill (Plate 1) south intermittently for 1 km. The sands in this unit are fine to very coarse-grained and display trough crossbedding and horizontal stratification.

Structure

The Sand Hill fault strikes approximately north - south with strikes ranging from N12°W to N23°E (Fig 3). The fault dips range from 70° E to vertical, with slickenside striae and stratigraphic separation indicating dominantly dip-slip motion (Fig 3). Slickenside striae plunge from 44° to 88° indicating a local component of sinistral or dextral strike-slip motion in addition to the dominantly normal motion (Fig 3). Within the study area, the fault zone width ranges from 1 to 10 m both along strike and vertically.

Displacement of units across the fault varies with age of the unit. The magnitude of displacement of each unit increases with the age of the unit, as is typical of growth faults. The uppermost unit (QTsacs; Table 1), deposited across the fault at the Red Hill (Plate 1), has been offset ~10 m by the fault. Offset of QTsacs indicates that motion along the Sand Hill fault occurred as recently as the Pleistocene. QTsas, (Table 1) the oldest unit exposed in the hanging wall, is locally folded into a syncline with a hinge ~20 m to the west of and parallel to the Sand Hill fault (Plate 1).

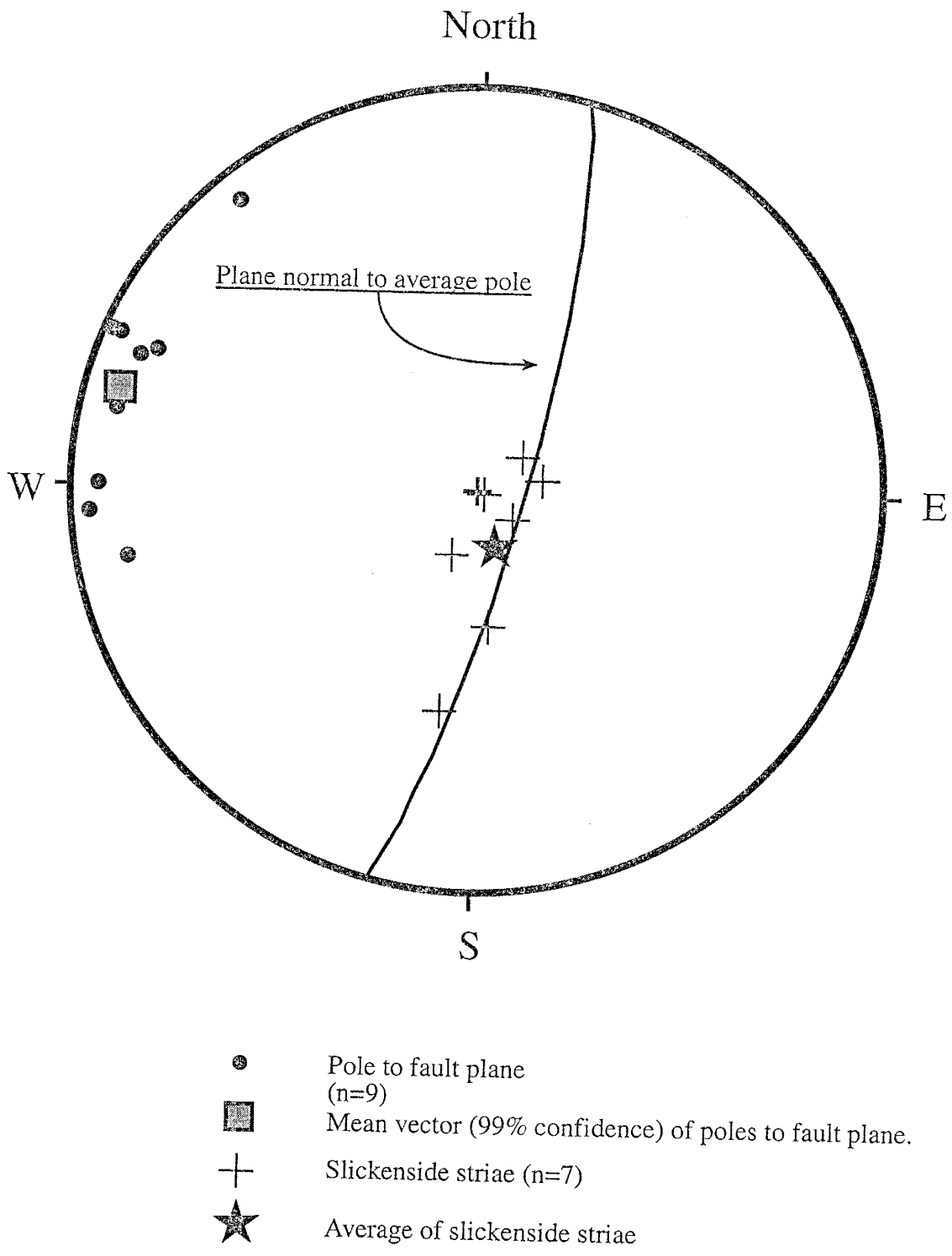

Figure 3. Lower hemisphere equal-area net plot of slickenside striae and poles to fault planes.

Cementation

The Sand Hill fault is preferentially cemented within the study area although the degree of cementation is highly variable (Plate 1). The width of the cemented zones ranges from a few millimeters to 6 m. The cement is dominantly sparry calcite where the cemented zone is greater than 25 cm wide and dominantly micritic calcite where the cemented zone is less than 25 cm wide. Different line types according to the width of the cemented zone (Plate 1) depict fault-zone cements within the map area.

The most obvious cementation pattern is that cements are almost exclusively confined to the hanging wall mixed zone; one exception, where the footwall is cemented for ~ 10 m along strike, exists along the 7.2 km stretch of the fault within the 1:6,000 map area. Note that the hanging wall is on the basinward side of the fault. Two other faults outside the map area, the Calabacillas to the east and the Pilares to the west, are also cemented on the basinward sides as indicated by reconnaissance mapping.

Oriented concretions are locally evident within strongly cemented portions of the fault zone. Within the map area, the flow features are largely sub-vertical and generally inclined to the slickenside striae in most areas of the fault zone (Fig. 4 and Plate 1).

Detailed Mapping

Methods

Two study sites were selected for detailed mapping at a scale of 1:100 and 1:400. These sites were chosen to characterize variations in fault-zone width and cementation with stratigraphy so that controls on fault zone width and fluid flow

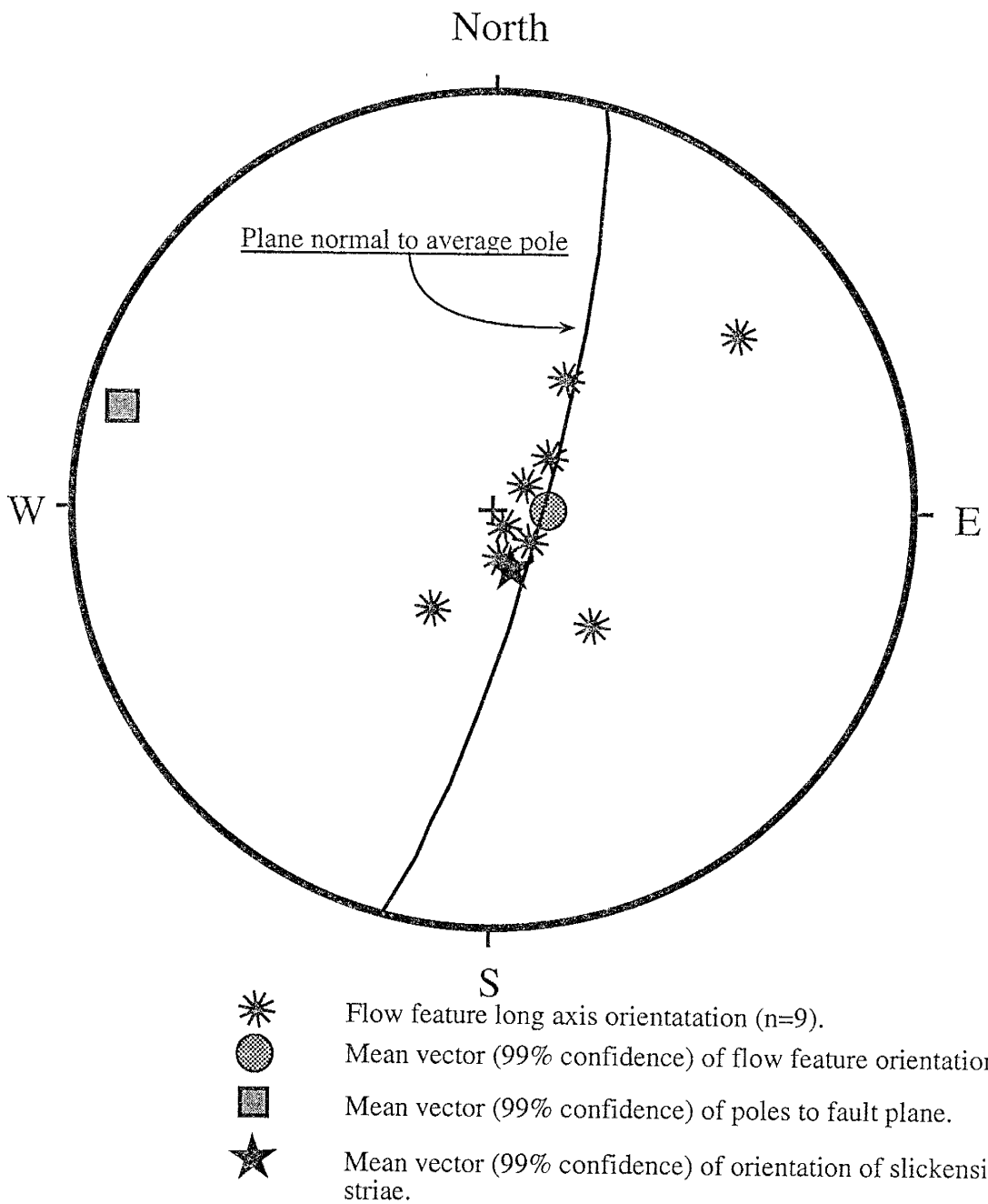

Figure 4. Lower hemisphere equal-area net plot of flow feature orientations showing relationships to structural features.

could be investigated. The southern site, the Shooting Gallery, was chosen because it is an area where the fault ranges from being narrow (2.5m) and poorly cemented to being moderately wide (10m) and well cemented. It also represents sections of the fault where thinly bedded clays and sands are juxtaposed against thickly bedded clays and sands. The northern site, the Waterfall, was chosen because it is an area where the fault ranges from moderately wide (15m) to very wide (20m) and is strongly cemented. It also represents portions of the fault where sediments on both sides of the fault are thickly bedded sands. A theodolite equipped with an electronic distance meter (EDM) was utilized to survey in fault-zone units and beds adjacent to the fault to create maps and cross-sections with an accuracy of ±5 cm.

Sedimentary units were divided on the basis of lateral continuity within the study site and relatively uniform grain size. A map and cross-section were prepared from the theodolite data. Due to the high angle of the outcrop at the Shooting Gallery site, the map was ineffective at showing the relationships within the fault zone and only the cross section is presented (Plate 2). Upon completion of the mapping with the theodolite, samples were collected from the fault-zone units and adjacent beds for grain-size analysis (see Appendix B for grain size analysis methods and data).

Fault-zone architecture and units

The Sand Hill fault zone can be divided into distinct domains on the basis of macroscopic structures: 1) footwall damage zone, 2) footwall mixed zone, 3) core zone, 4) hanging wall mixed zone, and 5) hanging wall damage zone (Fig. 5). This division is similar to that of previous workers (Sibson, 1977; Chester and

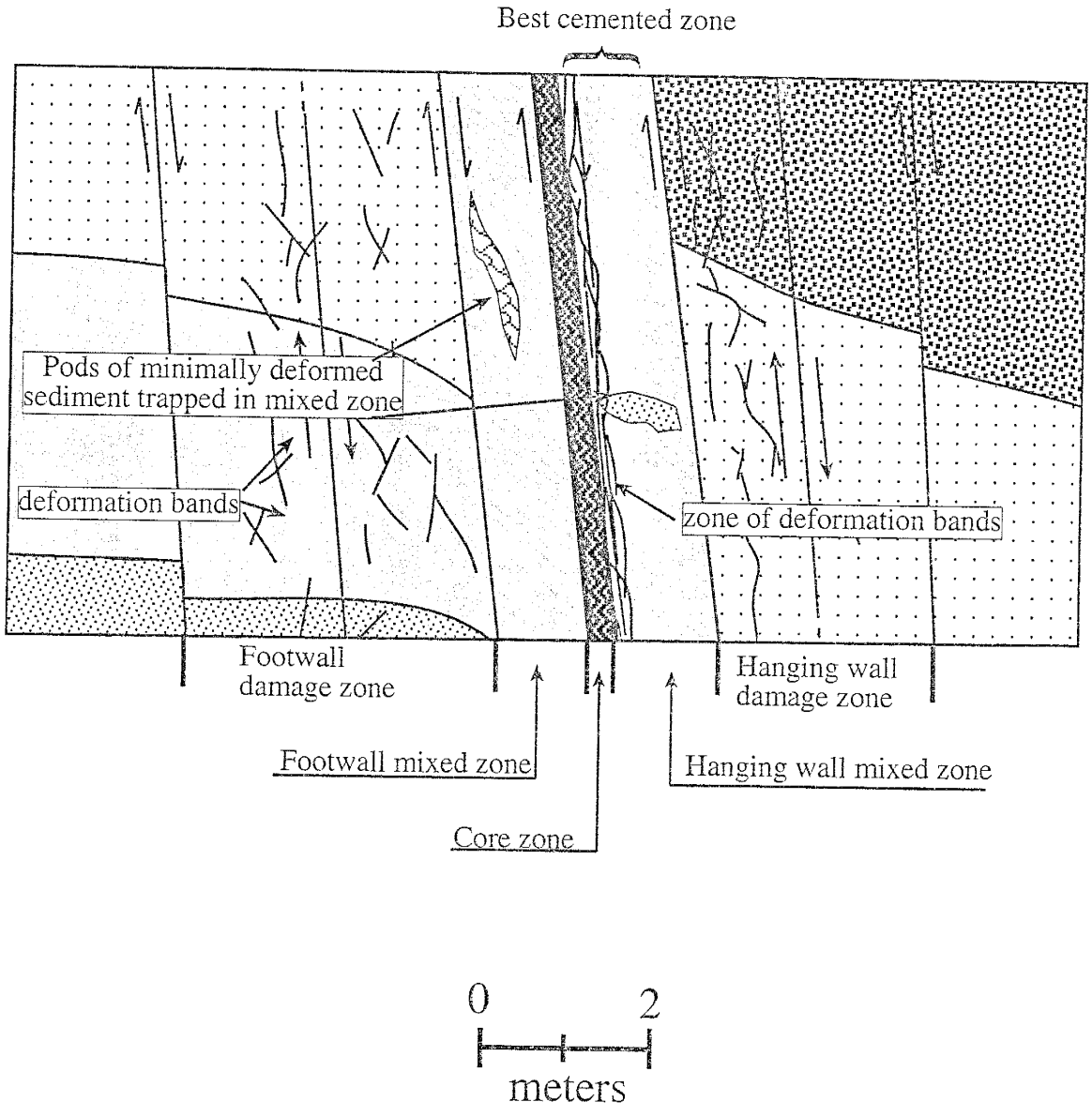

Figure 5. Schematic diagram based on photos of the fault zone at the Shooting Gallery site, showing main structural features and terms used for architectural elements.

Logan, 1986; Smith et al., 1990; Byerlee, 1993; Caine et al., 1996) with the exception of the mixed zones. Also, structures within the damage and core zones in these poorly consolidated sediments differ from those described in rock.

For the detailed mapping both the width of the fault zone in the hanging wall and the width of the fault zone in the footwall were measured. Hanging wall and footwall fault-zone widths were determined by measuring from the main slip surface to the boundary between the damage zone and intact bedding in the hanging wall and footwall respectively. Fault zone widths could be measured only where the fault zone and adjacent sediments were sufficiently well exposed to allow accurate determination of the boundaries without major excavation of the outcrop.

Damage zones

The damage zones extend from the first fault-related structure visible as the fault is approached to the boundary of the mixed zones (Fig. 5). The damage zones show evidence of minimal deformation. Deformation bands (cf. Aydin, 1978; also known as granulation seams Pittman, 1981; or cataclastic slip bands, Fowles and Burley, 1994) and small slip surfaces (cf. Aydin, 1978), are present in the damage zones (Fig. 6a+b). Many of these deformation bands and slip surfaces are preferentially cemented. Fractures and veins that are common features of damage zones in rock (e.g., Bruhn et al., 1994) are absent in these poorly consolidated sediments. The beds in the damage zones may also be dragged up to several meters along the boundaries with the mixed zones.

Figure 6a. Photograph of footwall damage zone with dragged bedding indicated by dashed line and deformation bands (d) highlighted (better shown in figure 6b). Mixed zone visible at right edge (M) bound by slip surfaces (S). Gray wall-like feature on right-hand side is cemented hanging wall mixed zone. Gray meter stick shown for scale. Photo was taken facing north at the Shooting Gallery bed #6.

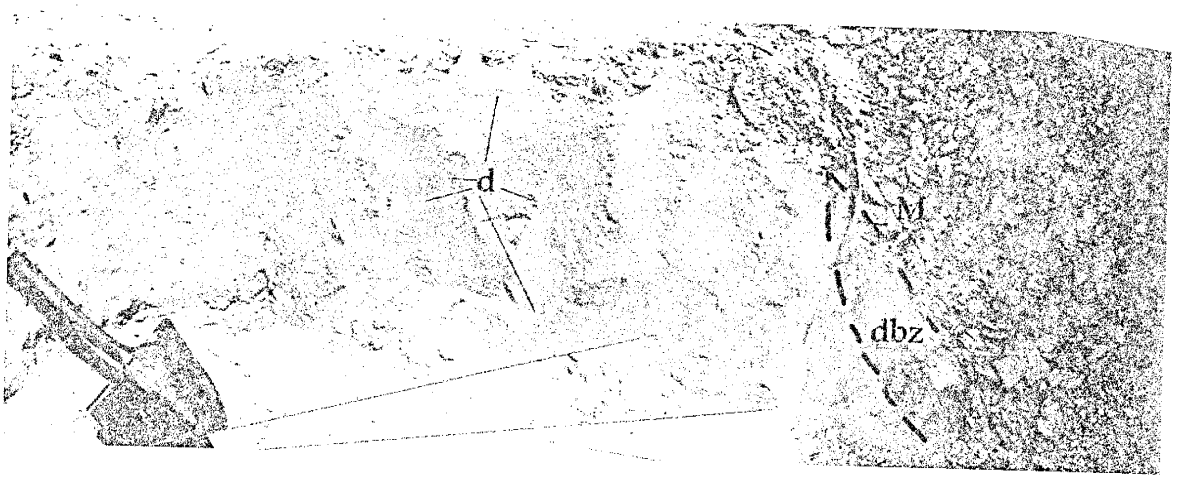

Figure 6b. Photograph of footwall damage zone with deformation bands (d). A zone of deformation bands (dbz) bounds the mixed zone (M). Shovel shown for scale. Photo was taken facing north at the Shooting Gallery.

Mixed zones

The mixed zones typically contain sediments that have undergone a structural change in which bedding is either overprinted by a deformational fabric or is completely destroyed through tectonic mixing. The change from intact sediment to tectonically mixed sediment is transitional, with the degree of mixing generally increasing as the core-zone / mixed-zone boundary is approached. For the purpose of mapping, I defined the mixed zone by offset of bedding greater than bed thickness along a slip surface subsidiary to the main fault (Fig. 5). It was defined as such because if there has been displacement greater than bedding thickness then a juxtaposition of different units exists which can have an important impact on fluid flow. Also, although the degree of mixing is transitional, no grain-scale mixing is observed to occur until a displacement of at least ~1m or average bed thickness has occurred. The mixed zones are composed of material derived from beds that have been transported past the zone during slip. The mixed zones contain dragged and extended beds, multiple slip surfaces, and areas of tectonically mixed sediment (Figs. 6, 7, & 8). A zone of deformation bands, ~2 - 10 cm wide, commonly exists immediately adjacent to the core-bounding slip surfaces in the hanging wall mixed zone.

The incorporated sediment ranges in degree of deformation from rootless pods of intact bedding, to highly attenuated beds, to tectonically mixed sediment (see maps, Appendix A). The attenuated beds are thinned, commonly forming 1-10 cm wide ribbons that define a foliation. Tectonic mixing is accomplished by slip, drag, and grain-scale mixing forming a sand pebble mix in a clay matrix (Fig. 8).

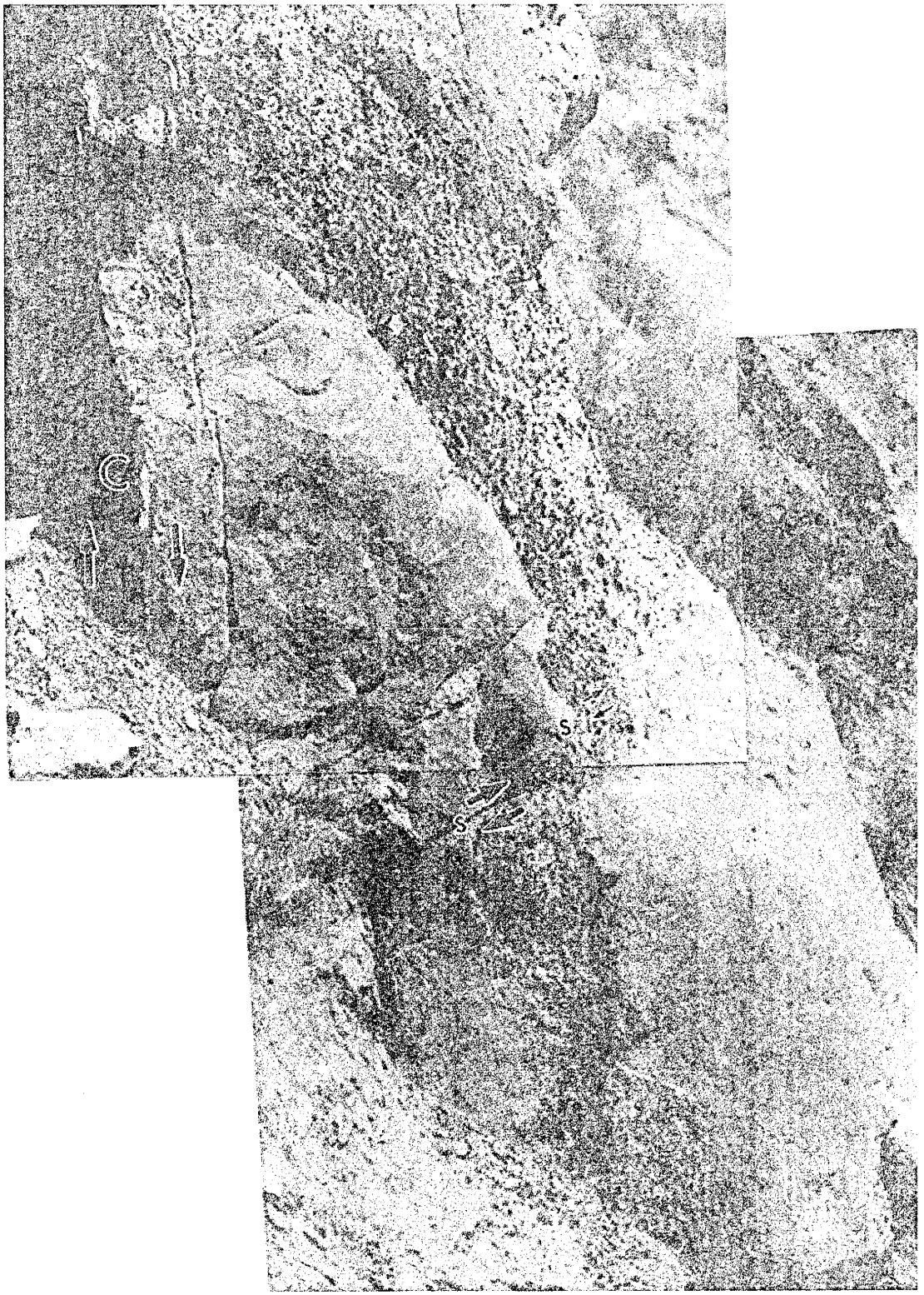

Figure 7. Photograph of cemented hanging wall mixed zone. Gravel bed exhibits pinch and swell boudinage. Boudins are offset by minor synthetic slip surfaces (s). Core zone (C) is on left. Cemented portion is ~1m wide. Photograph was taken facing north at Shooting Gallery.

Figure 8. Photograph looking down at an oblique angle on the footwall mixed zone showing sediments that are extended and locally have undergone grain-scale mixing. Foliation in mixed zone is defined by compositional banding. One strand of the core zone is exposed (C). Cemented wall at top of photo is hanging wall mixed zone. Arrows define sense of fault motion along core zone (C). The flag and wire in photo are ~.25m tall for scale. Photo was taken facing east where fault strikes north-south.

Where the incorporated beds are variable in composition, e.g. a gravel bed surrounded by sand, boudinage may be evident (Fig. 7). The degree of deformation of beds appears to increase from the damage-zone / mixed-zone boundary to the mixed-zone / core-zone boundary. As the core-zone boundary is approached, thinned beds are often rotated into a sub-parallel orientation with the fault and may exhibit a foliation. The foliation is usually defined by compositional layering on the scale of .5 to 10 cm and / or by the elongate axes of sand grains and pebbles (Figure 17; Goodwin and Haneberg, 1996), and / or by alignment of clay. Original sedimentary textures such as cross-bedding, imbrication, grading, etc. may be completely destroyed through tectonic mixing.

As mentioned previously, the hanging wall mixed zone may be preferentially cemented. The hanging wall mixed zone is well cemented only when the mixed-zone sediments are relatively coarse sands and gravels.

Core zone

The core zone ranges from a few millimeters to several centimeters in thickness and is bounded by slip surfaces. It may be composed of multiple slip surfaces separated by foliated clays and sands (Fig. 9). The strongly foliated clays form a veneer that is continuous over extensive distances both vertically and laterally; where it is absent, the gap is in most places less than 30 cm in length (Fig. 9). Cementation of the core zone is limited and where present is restricted to foliated sand.

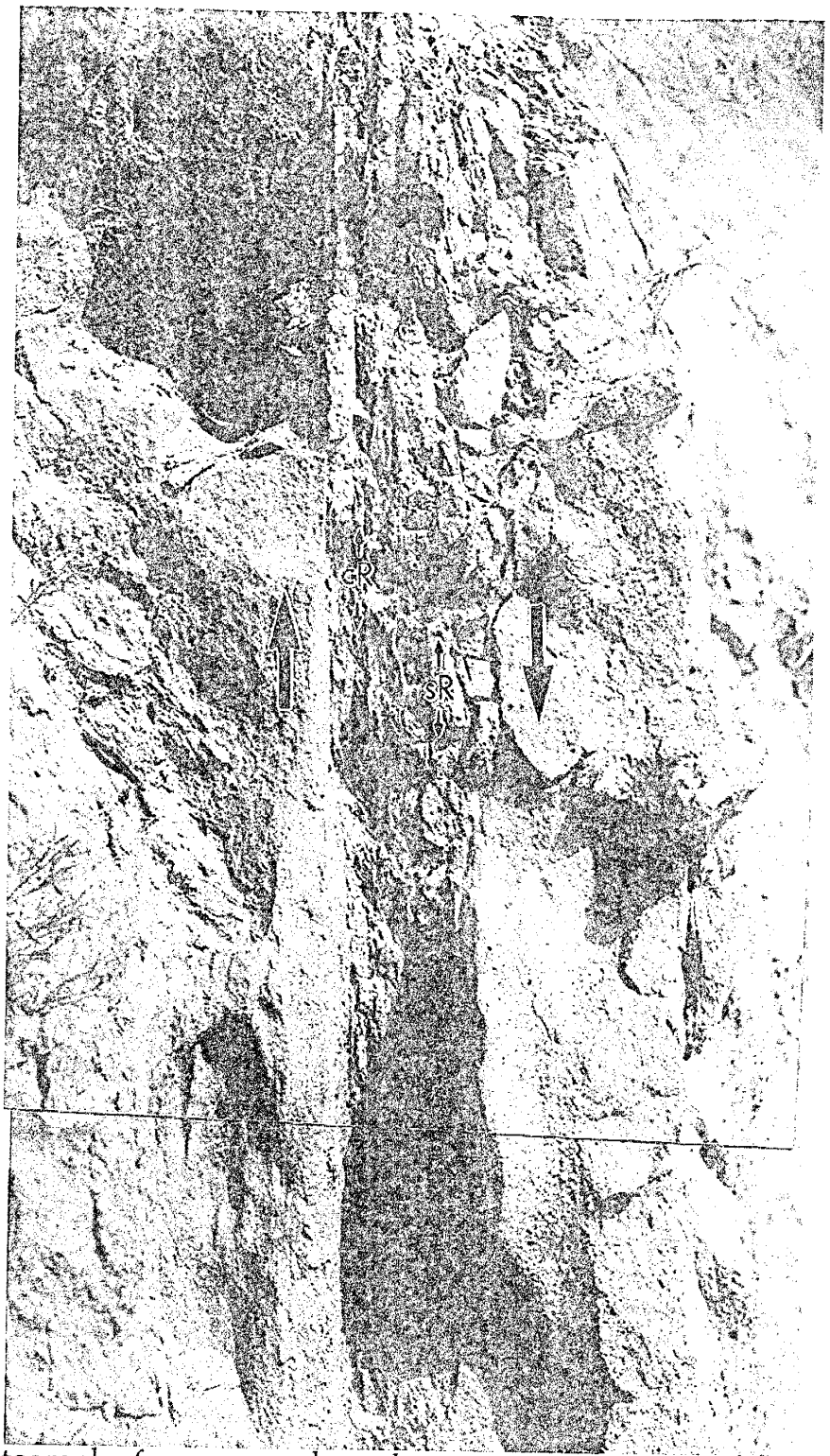

Figure 9. Photograph of core zone where clay veneer is poorly developed (top) to absent (bottom). Sand ribbons (sR) and clay ribbons (cR) are indicated. The adjacent hanging wall sediments, hanging wall mixed and damage zones (right side of photo) are sand-rich. Fault-parallel foliation is defined by compositional banding of clay, sand ribbons, and aligned clays. Photo was taken facing north at the Shooting Gallery. Photo is 1 m from top to bottom.

Shooting Gallery: narrow to moderately wide, variably cemented fault zone

The Shooting Gallery site (Plate 1) was chosen for study because it represents areas along the fault where sand is juxtaposed against both clay and sand, and thick beds are juxtaposed against thin beds. The total fault zone width, including footwall and hanging wall mixed and damage zones, ranges from 2.5 to 10 m. The fault zone is poorly cemented where it is narrow and well cemented where it is wide. The fault and adjacent sediments are well exposed within an ~45 m vertical section of the greatest vertical exposure along the fault. All three units of the Sierra Ladrones formation are exposed in the hanging wall. A series of relatively thin (1-3 m) beds of fine sand and clay of the Zia formation are exposed in the footwall.

A relationship between fault zone width and grain size is evident within the hanging wall (Plate 2). Where the hanging wall fault zone is wide, the adjacent hanging wall units are coarse-grained sands and gravels with very minor amounts of clay. The fault narrows at the unconformity between QTsas and QTsams, coincident with a change from 3%-5% clay to 42%-62% clay in adjacent beds (Plate 2). The differences in width are largely accommodated by variations in damage zone width; the mixed-zone widths are relatively constant and do not appear to correlate with either mean mixed-zone grain size or adjacent bed grain size.

Cementation of the hanging wall mixed zone also appears to be related to the grain size of the adjacent sediments. The hanging wall mixed-zone cements are several meters wide below the unconformity where the adjacent sediments are sands and gravels and are narrow and poorly developed above the unconformity where the adjacent sediments are fine-grained and clay-rich (Plate

2). Where the cemented zone is wide, it is well cemented with sparry calcite. The cement is best developed immediately adjacent to the core zone and becomes less well developed with increasing distance away from the core zone / mixed zone boundary. Where the cemented zone is narrow and poorly developed it consists of micritic calcite; in these areas, the cement is patchy and present mainly adjacent to the slip surface on the boundary between the core and hanging wall mixed zone. The cemented zone is widest and best developed where the hanging wall sediments are coarse-grained. It is observed that the cements are best developed where both footwall and hanging-wall sediments are coarse-grained sands and gravels.

Some variation in fault-zone width exists within the footwall but the correlation with the adjacent sediment type is not as obvious as in the hanging wall. Overall, the footwall fault zone width is similar to the width of the hanging wall where it is narrow and adjacent to clay-rich sediments. If the grain size of adjacent sediments is plotted against fault-zone width for both hanging wall and footwall it appears that the width increases where the adjacent sediments are at least 82% sand (Fig. 10). This relationship isn't entirely consistent in the footwall, as there are beds with at least 82% sand yet the fault is narrow. Also, there are beds with 18% or more clay and silt that correlate with a small increase in fault-zone width, although these beds are mostly thin and sandwiched by beds with more than 82% sand. Cementation in the footwall is minor relative to the hanging wall, and where present is generally confined to small-displacement faults and deformation bands within the damage and mixed zones.

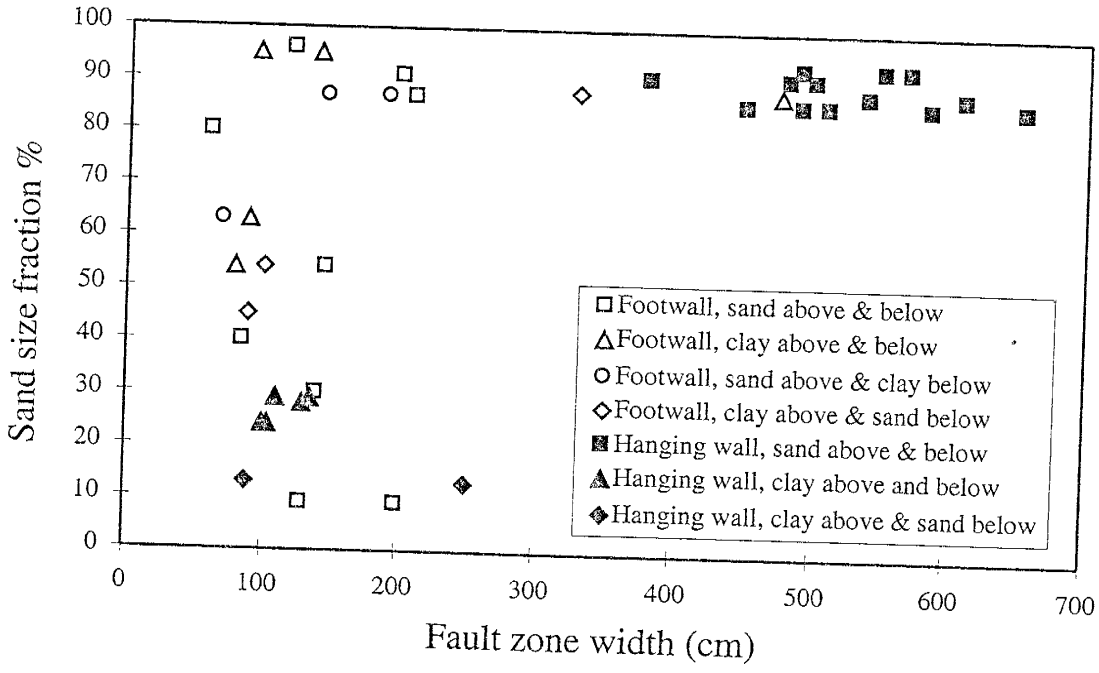

Figure 10. Plot of fault zone width vs. grain size of adjacent sediments. The fault zone remains relatively constant in width until the sand content is >82%, at which point the fault zone widens dramatically. To help determine whether a single bed or multiple beds influence the fault zone width at any point, points were plotted according to their stratigraphic context: i.e. sand above and below.

The core zone of the fault is .5 cm to 40 cm wide and is mainly composed of a .3 to 32 cm wide strongly foliated clay veneer (Fig. 11). In some areas, the core zone is composed of multiple thin clay veneers and foliated ribbon-shaped bands of sand that define a foliation (Fig. 11). The clay veneer is continuous along the fault zone with the exception of two gaps, both <30 cm in vertical extent. Cementation of the core zone is generally confined to foliated sand ribbons where the clay veneer is thin. The cements are sparry calcite where well developed and micritic calcite where poorly developed.

Waterfall study site: wide and well cemented fault zone

The Waterfall site was chosen as representative of the many locations along the fault where the fault zone is wide, strongly cemented, and has multiple splays and bends. The Waterfall site lacks the vertical exposure that the Shooting Gallery has, but offers good along-strike exposure. Due to the lack of vertical exposure, it is more difficult to relate fault-zone characteristics to sediments immediately adjacent to the fault. A map (Plate 3) was constructed at a scale of 1:400 to illustrate the spatial variability of the structures and units within the fault zone. Two cross sections (Figs. 12 & 13), both constructed at a 1:100 scale, show vertical variation of features within the fault zone and the relationship of fault-zone structures to the adjacent sediments.

The lack of exposed strata adjacent to the fault is a result of fault-parallel erosion. Many of the characteristics of the sedimentary beds adjacent to the fault, however, can be inferred from a nearby section with ~30 m of vertical exposure. The variation in composition between different sedimentary units in the

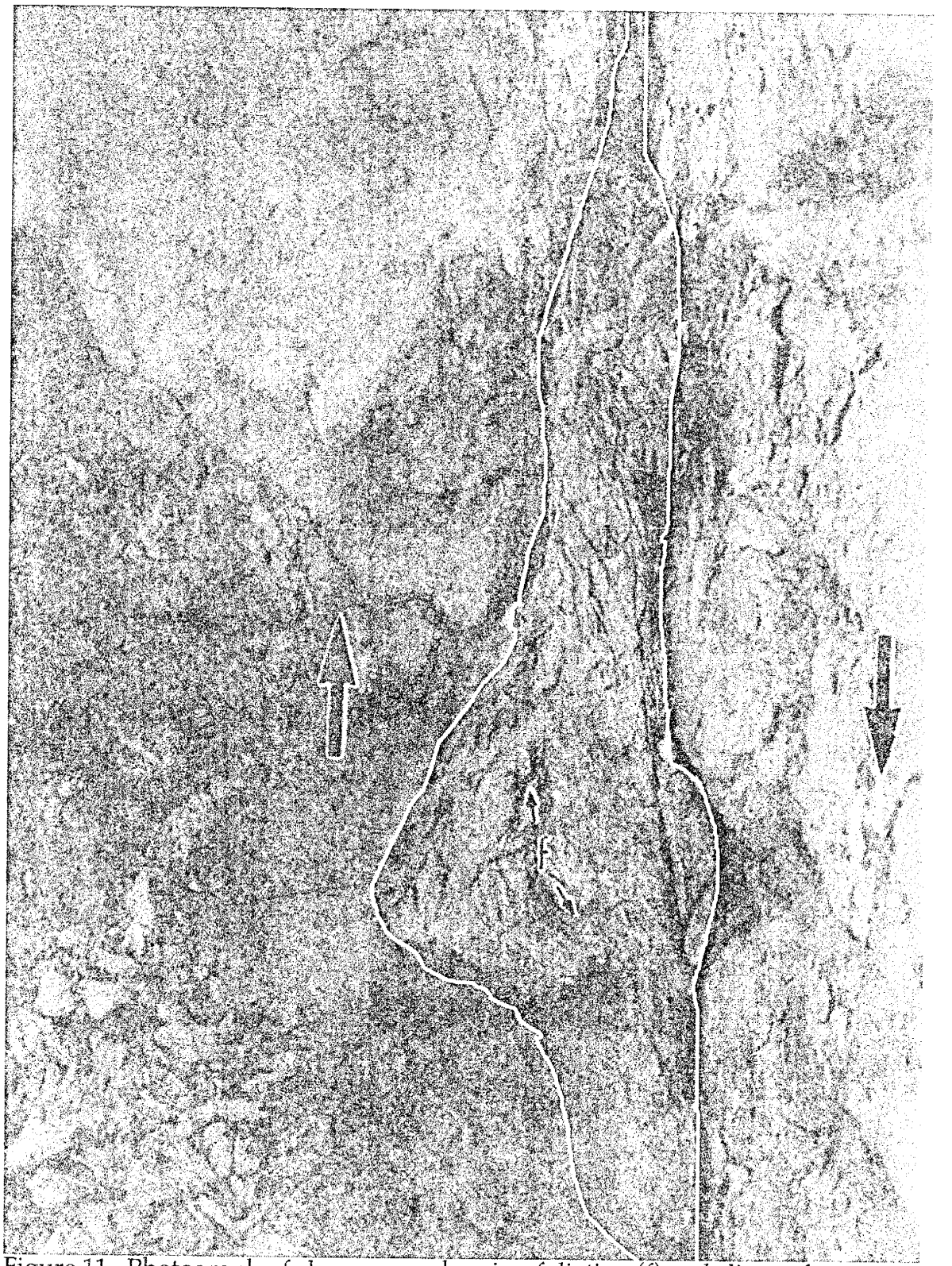

Figure 11. Photograph of clay veneer showing foliation (f) and slip surfaces, white lines, (s). Photo was taken facing north at bottom of Shooting gallery. Hand at left edge of photo for scale.

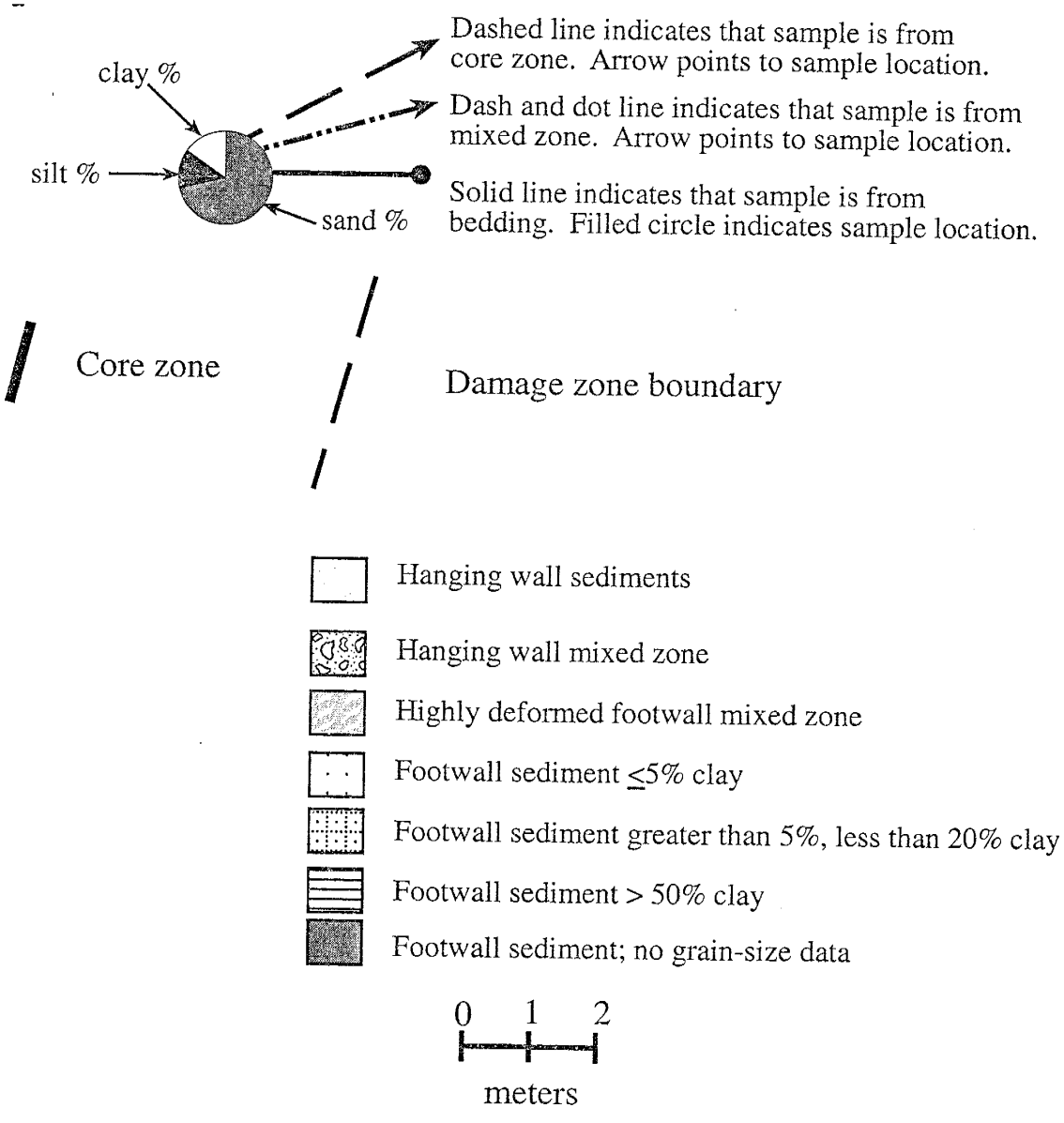

Key and scale for figures 12 and 13.

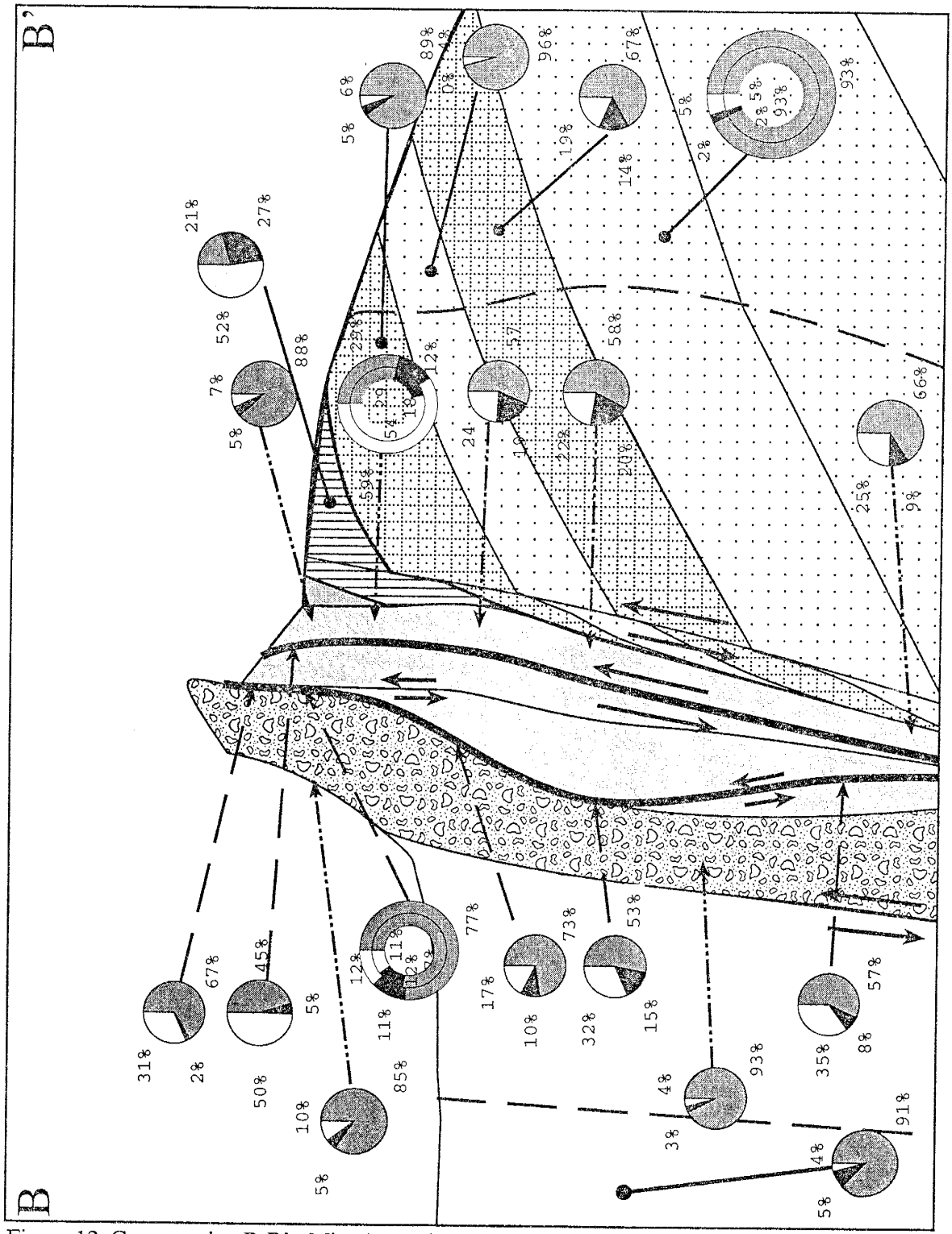

Figure 12. Cross section B-B'. Mixed zone is highly deformed and original bedding is nearly destroyed by tectonic mixing. Double-ringed plots are duplicate samples to check accuracy of grain-size analyis.

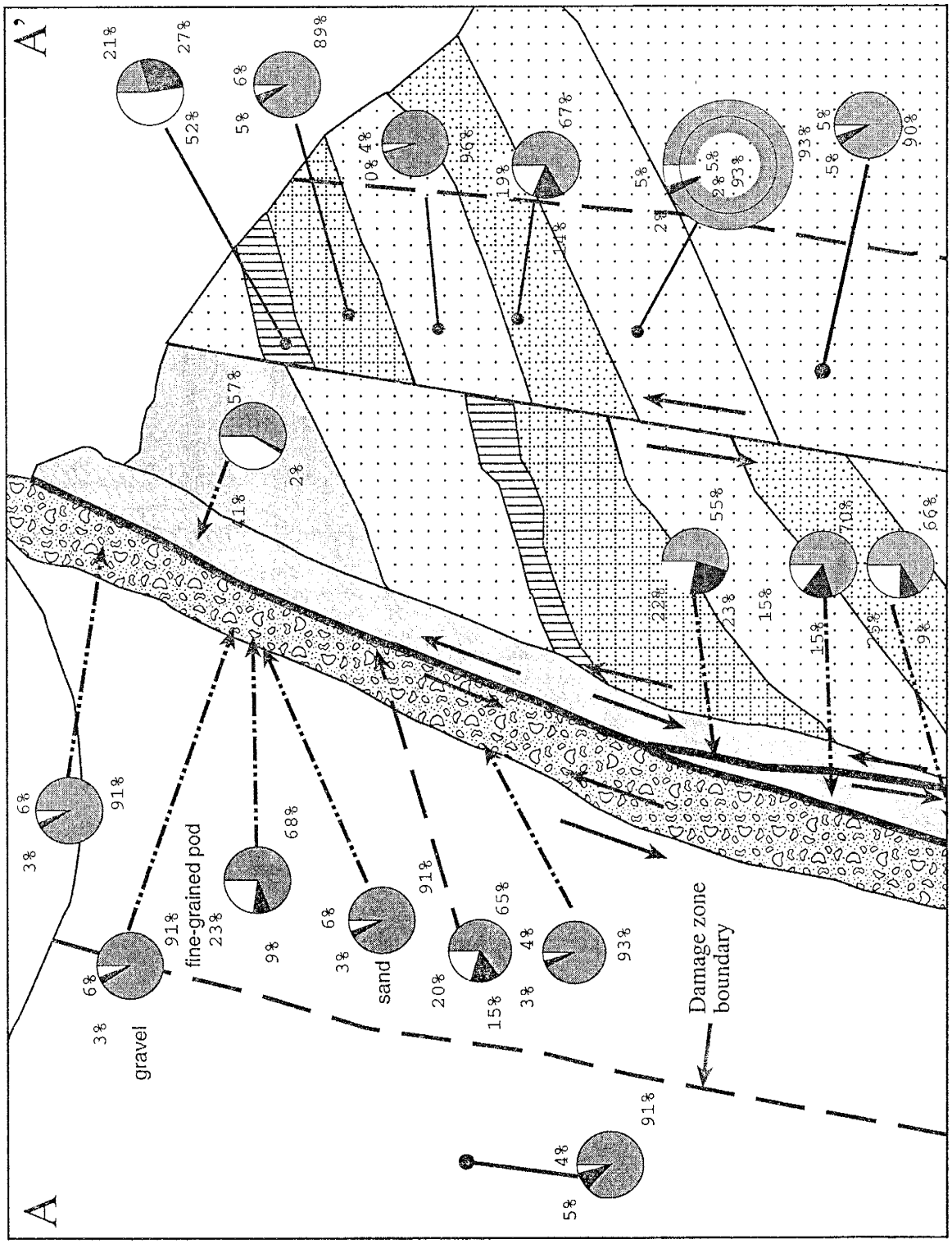

Figure 13. Cross section A-A'. Majority of mixed zone is defined here by the displacement >average bed thickness criterion since sediments are minimally deformed except adjacent to the core zone.

Shooting Gallery is absent in the Waterfall area. The sediments in the Waterfall site are less clay rich and beds are thicker, resulting in a relatively compositionally homogenous section.

The hanging wall sediments include the upper and middle units of the Sierra Ladrones Formation. The upper unit consists of coarse sands and gravels. The middle unit is more sand rich at the Waterfall site than at the Shooting Gallery site. At the Waterfall site, it is a well sorted unit of fine- to medium-grained sands and thin gravel interbeds that are locally strongly bioturbated resulting in a homogeneous texture.

The footwall sediments are eolian and fluvial Zia Formation sands. The majority of exposed sediments are fluvial, trough cross-bedded, medium- to coarse-grained, medium to well sorted sands. In the stratigraphically lowest exposure a thickly bedded, well sorted, eolian, cliff-forming unit is exposed. Adjacent to and above the fault exposure, three clay beds less than 25 cm thick were found. The footwall section has several laterally continuous, preferentially well cemented beds outside the fault zone. These beds are cemented with a combination of phreatic and vadose zone cements (Beckner, 1996).

At the Waterfall site, sediments cut by the fault contain very little clay. The fault zone is 1.5 to ~10 times wider than at the Shooting Gallery site. The damage zones account for the majority of the fault zone width. The width of the mixed zones is relatively constant with the exception of fault zone bends, where the mixed zones are wider (Plate 3). At these bends, the core zone of the fault bifurcates and large pods of relatively intact sediment are incorporated into the mixed zone. The incorporated sediment is compositionally distinct from the sediments exposed adjacent to the fault in either the footwall or hanging wall.

The damage zones are difficult to trace continuously on either side of the fault due to erosion and surficial cover, but are identifiable in enough areas to be mappable. Minor changes in width may have been overlooked due to poor exposure. The damage zone widths remain relatively constant throughout the Waterfall site.

The mixed zones in the Waterfall area are more complex than those in the Shooting Gallery (Fig 12 & 13). The footwall mixed zone includes many pods or slivers of footwall-derived sediment that are compositionally different and contain more clay than beds immediately adjacent to the fault exposure (Fig. 12, 13, & 14). Commonly these pods are bound by slip surfaces and exhibit a foliation that is sub-parallel to the fault as can be seen in Figure 15. This foliation can be used as a kinematic indicator and show the sense of shear. The edge of the footwall mixed zone consists of a zone of deformation bands that progress into a series of small displacement slip surfaces and ultimately into a large displacement slip surface (Fig. 16). The footwall mixed zone is considerably wider than at the Shooting Gallery. The footwall mixed zone ranges from being highly mixed and exhibiting a strong foliation to being composed of relatively intact bedding displaced greater than the bed thickness (>2 m) to having a narrow zone of highly mixed sediments near the core zone. The hanging wall mixed zone doesn't display the same degree of tectonic mixing as the footwall. The hanging wall mixed zone contains sediments that have more gravel than do beds outside of the mixed zone. The gravel-rich sediments incorporated in the hanging wall mixed zone compositionally resemble gravel beds of the lower unit of the Sierra Ladrones formation.

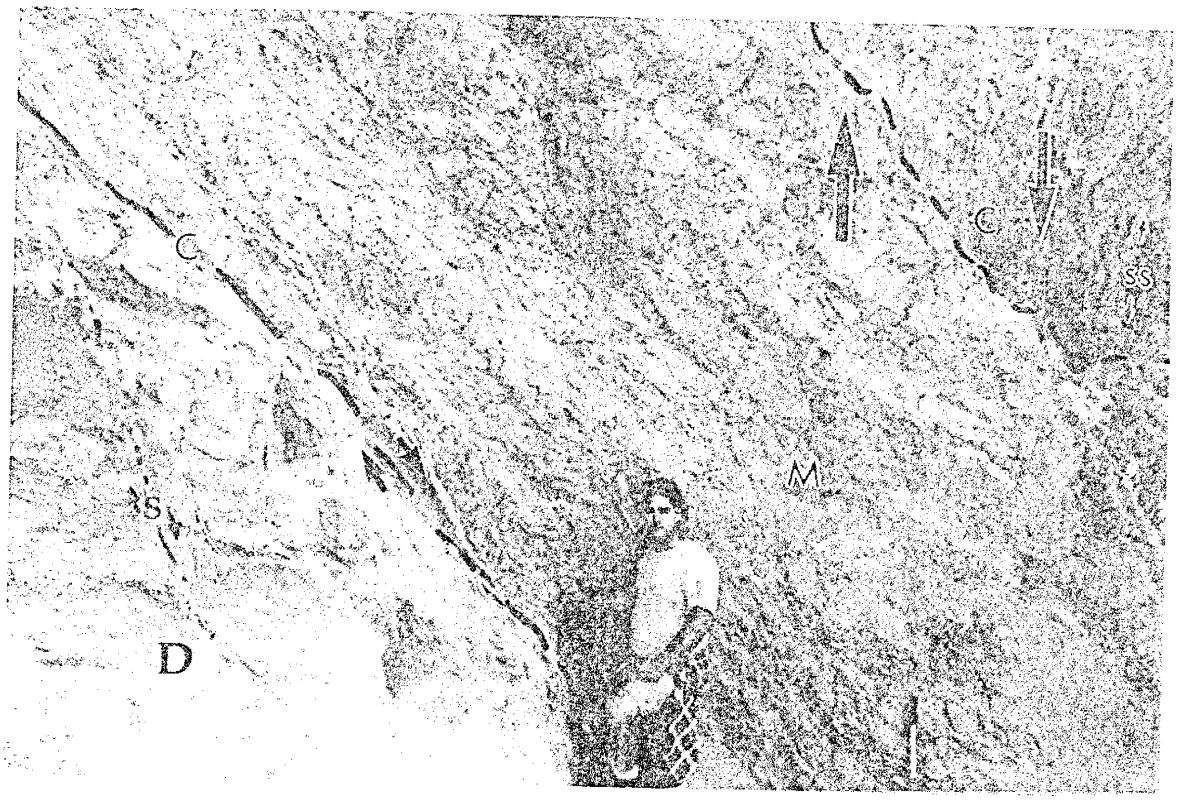

Figure 14. Footwall mixed zone (M) contains numerous extended beds surrounded by zones of grain-scale mixing. Extended beds define a foliation that is sub-parallel to the bifurcated strands of the core zone (C). Damage zone (D) contains small-displacement slip surfaces (s). Cemented wall in upper-right hand of photo is hanging wall mixed zone and has sub-vertical slickenside striae (ss). Photo was taken facing southeast at the Waterfall site. Chris Dimeo for scale. Viewed looking east toward fault.

Figure 15. Photograph of portion of footwall mixed zone ~5m south of figure 14. Foliation (F) is inclined to slip surfaces (S). The direction of inclination is reflects the sense of shear between slip surfaces (S). Photo was taken facing south. From left to right of photo is ~.75 m.

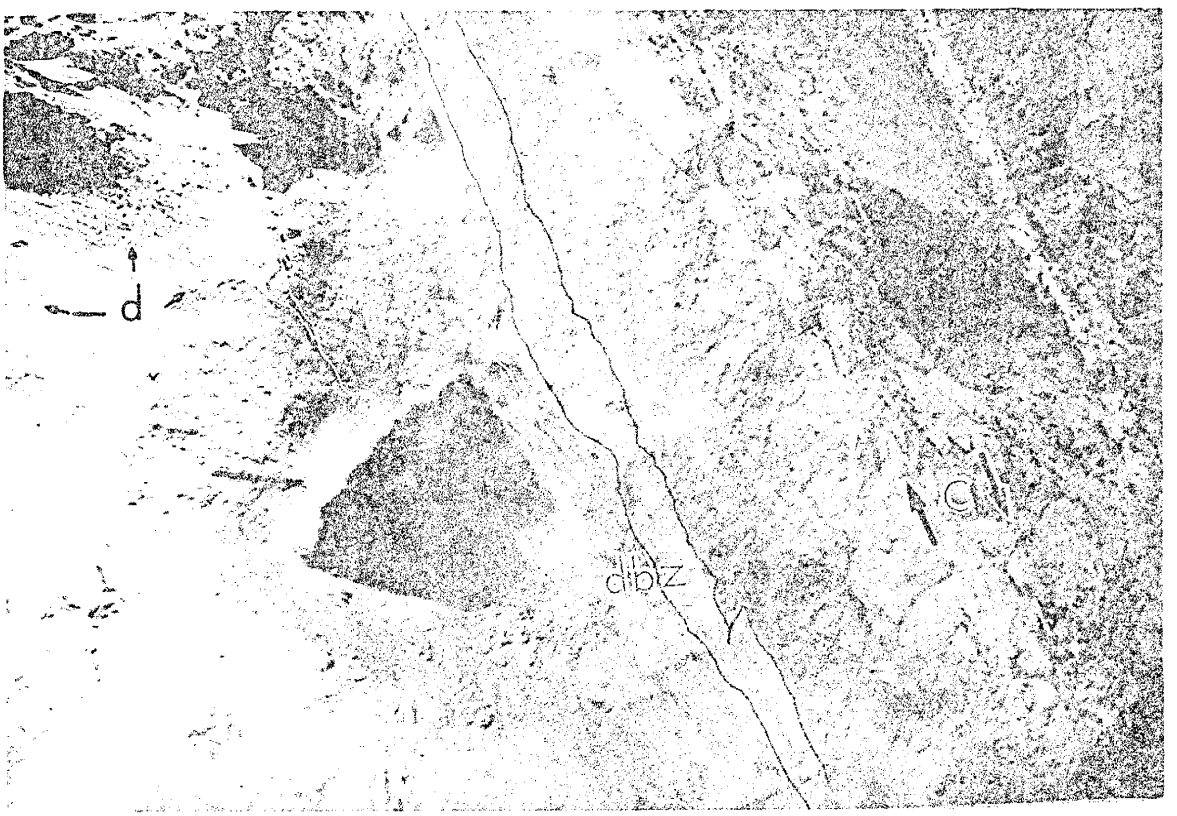

Figure 16. Photograph of portion of footwall mixed zone shown in figure 14 illustrating transition from single deformation bands (d, highlighted in white) to a zone of deformation bands (dbz, outlined in black) to small displacement slip surfaces (s) to a through going large displacement slip surface which is a strand of the core zone (C). The zone of deformation bands is oriented parallel to bedding rotated parallel to the fault. Photo was taken facing north. From left to right of photo is ~.50 m.

The gravel beds are minimally deformed except immediately adjacent to the core zone where they are dragged and rotated into parallelism with the fault (Fig. 17).

The core zone in the Waterfall area is more complex than at the Shooting Gallery site. The core zone bifurcates into multiple strands isolating pods of mixed sediment between the strands. The clay veneer in the core zone is less developed than at the Shooting Gallery and contains more small gaps.

The degree of fault-zone cementation is greater at the Waterfall site than at the Shooting Gallery. The majority of the hanging wall mixed zone exposure is strongly cemented and the cemented zone is commonly greater than 2 m wide. The fault zone cements are, as in nearly all exposures of the Sand Hill fault, largely confined to the hanging wall (basinward) mixed zone, diminishing in degree of development into the hanging wall damage zone. The cements locally form oriented flow features along the margin of the cemented zone next to the damage zone. The orientations of the flow features are subvertical with the exception of the area where the fault bends, in which the orientations range from vertical to nearly horizontal.

Discussion

The width of the Sand Hill fault zone generally correlates with the grain size of the adjacent faulted sediments. The fault zone is narrow where there is either a thick section of sediments with $\leq 82\%$ sand, (Fig. 10) or where a sub-equal number of thin, alternating, clay- and sand-rich beds exist. This is best seen at the Shooting Gallery (Plate 2).

Figure 17. Hanging Wall mixed zone gravels at Waterfall site that are rotated into parallelism with the fault core (c). Thin arrows show alignment of pebbles and indicate rotation of orientation. Outcrop width in photo is ~.5 m.

Here the footwall sediments are composed of relatively thin alternating clay- and sand-rich beds that are roughly sub-equal in number, and the fault zone is narrow. It is also narrow in the hanging wall where a thick sequence of clay-rich beds correlates with a dramatic thinning of the fault zone. The fault zone is wide where the adjacent sediments are coarse-grained, clay-poor, and thickly bedded as best seen in the Waterfall site where the fault zone is substantially wider than at the Shooting Gallery. Here the beds are coarse grained in both hanging and footwalls with little clay present in the entire footwall section (only two beds contain a substantial amount of clay and they are $\leq$ 25 cm thick).

The relationship between grain-size and fault-zone width is generally consistent. Two exceptions to this relationship exist: 1) where clay-rich beds are bordered by sand-rich beds there is a small increase in fault-zone width in the clay bed, and 2) where thin sand-rich beds are bound by thin clay-rich beds the fault zone is narrower, as seen at the Shooting Gallery (Plate 2). This relationship may be due to a combination of processes including strain hardening, strain softening, and bed-parallel slip. Whether one or all of these processes are active in any given bed cut by the fault may be dependent on the clay content of the beds. Also the width of the fault zone may be dependent on which process was active, as some processes would result in a wider fault zone and others in a narrow fault zone. In order to better evaluate whether these processes explain variations in fault-zone width at the Sand Hill fault each is reviewed and discussed in terms of the Sand Hill fault.

Strain Hardening

Strain hardening is a process that can make a fault zone wide (e.g., Aydin and Johnson 1978; Aydin, 1978). Strain hardening makes it energetically more favorable to deform material adjacent to a previously strain-hardened structure instead of reactivating it. This results in the formation of numerous structures and widening of a fault zone during subsequent deformational events.

Strain hardening is reported to occur in crystalline rock under special circumstances; Morrow et al., 1982; Marone et al., 1990), sandstone (Aydin and Johnson 1978; Aydin, 1978; Fowles and Burley, 1994), and particulate media (Frydman, 1976). Particulate media, such as unconsolidated sand, are mechanically distinct from low porosity rock. Brittle failure of low-porosity rock causes a transient positive dilatancy resulting in the opening of cracks and asperities along which a fault may form (Rudnicki, 1977). This typically results in a zone of weakness which prevents strain-hardening from occurring unless the gouge formed strain hardens. This is different than deformation of particulate media, in which strain will ultimately result in a negative dilatancy after a sometimes transient positive dilatancy (Borg et al., 1960). The negative dilatancy is caused by a tighter packing of grains and grain-size reduction. The tighter packing of grains is responsible for the increase of strength or strain hardening.

Strain hardening in sandstone is attributed to increased grain contact friction as a result of cataclasis. Cataclasis results in an increase in the number of grain contacts through grain-size reduction, greater grain interlocking, and a decrease in porosity. Preferential mineral precipitation along a strain-hardened structure may further increase its strength (Fowles and Burley, 1994). In the

faulted sandstones studied by Aydin and Johnson (1978), it is observed that a progression exists from a single deformation band to a zone of deformation bands to a larger displacement slip surface. The formation of a zone of numerous closely spaced deformation bands with similar orientations suggests that the strength of each deformation band is greater than the undeformed sediment adjacent to it indicating that strain hardening has occurred. In Aydin and Johnson's (1978) model, the zone of deformation bands will ultimately give way to a throughgoing slip surface along which repeated movements may occur.

The progression from a single deformation band or a zone of deformation bands to a slip surface is commonly seen within the Sand Hill fault zone (Fig 16). This progression only exists where sand-rich units are adjacent to the fault. This may imply that strain hardening was an active factor in the deformation process where sands were faulted. This indicates that the strain-hardening processes, which control fault-zone development in sandstone, may have occurred in the poorly consolidated sand-rich sediments cut by the Sand Hill fault.

Strain softening

Maltmann (1987) demonstrated in a series of experiments that intense repeated slip in argillaceous sediments can be accommodated within very narrow, discrete shear zones. This experimental observation is supported by the field evidence of Caine et al. (1996), who suggest that a higher degree of strain-localization occurs where a fault cuts a shale-rich protolith. Antonellini and Aydin (1995) measured fault zone width, which inversely correlated with clay content (Fig. 18). These observations are similar to observations of the Sand Hill fault: the fault zone is narrowest where it cuts clay-rich sediment.

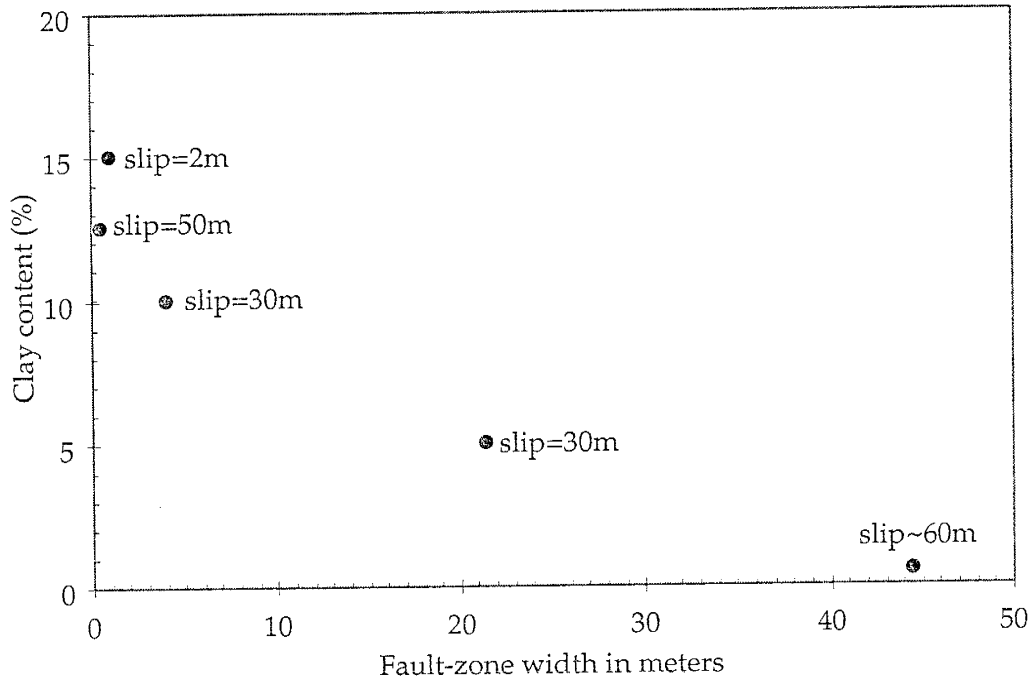

Figure 18. Plot of fault-zone width vs. clay content for faults in sandstone. Amounts of slip are indicated for each fault; no relationship between displacement and width is evident. A strong relationship between clay content and width is evident. Plot is from data presented in Table 3 of Antonellini and Aydin (1995).

Strain softening may be used to explain these observations. Strain softening results in a structure that is weaker than the undeformed material. Because a strain-softened structure is weaker than the adjacent sediments or rocks it will be preferentially reactivated in later events because it is energetically more favorable to reactivate a strain-softened structure than to create a new surface. This results in a narrow fault zone. Strain softening may explain the width of the Sand Hill fault zone where it cuts clay-rich units (Skempton, 1942). For repeated slip to be accommodated in a narrow zone, strain softening may have occurred.

Bed-parallel slip

Bed-parallel slip, flexural-slip folding, or quasi-flexural folding of strata adjacent to a fault zone can help contribute a significant quantity of material to the fault zone; which may increase the fault-zone width. Folding is commonly associated with faulting of rocks and sediments and may continue throughout a fault's history (Barnett et al., 1987; Cooke and Pollard, 1996; Watterson et al., 1998). Bed-parallel slip is an important factor in flexural-slip folding and is typically partitioned into shale rich layers that are sandwiched between more competent sand layers (Donath and Parker, 1964; Gibson, 1994; Pollard and Cooke, 1997; Watterson et al., 1998; Foxford et al., in press). Bed-parallel slip can add complexity to fault surfaces and cause asperities on the fault surface by creating steps between beds (Watterson et al., 1998). These steps may be later removed by faulting, contributing material to the fault zone.

Where sand units undergo flexural-slip folding it is expected that there would be a greater increase in fault-zone width than where clay-rich or shale

layers undergo flexural-slip folding. The sandstone units contribute more to the fault-zone width because they behave more competently causing them to be faulted and incorporated into the fault zone as intact pods or blocks (Gibson, 1994; Watterson et al., 1998). The shale or clay layers contribute less to the fault-zone width because they are typically thinned through smearing along the fault. In areas of a fault zone where strata have been rotated into sub-parallelism with the fault, bed-parallel slip can have a strong influence on fault-zone thickness, although bed thickness can also have a strong influence. If a thin clay bed sandwiched by two thicker sand beds were rotated and incorporated into the fault zone through flexural-slip folding, bedding-parallel slip and thinning would occur along the clay bed with the deformation being distributed throughout the entire clay bed forming a clay smear (e.g., Foxford et al., in press). With continued displacement and increased slip along bedding planes the clay layer would continue to thin and accommodate bedding-parallel slip and would begin to wear and narrow whereas the more competent sand layers would retain their original thickness to the fault zone. Where the case is reversed, and a thin sand is sandwiched between thick clay layers, bedding-plane slip along the clay-sand boundaries would be expected. This may cause the sand to form an asperity in the fault plane which may be removed during later faulting. The clay beds would be smeared and thinned through continued faulting resulting in a relatively narrow fault zone with small intact pods of the thin sand layer as seen in fault studies of Gibson (1994).

Flexural-slip folding of adjacent strata into parallelism with the fault plane may have occurred at the Sand Hill fault (Fig. 6, 16, and 19). Preliminary observations indicate in some areas that where the adjacent strata is thickly

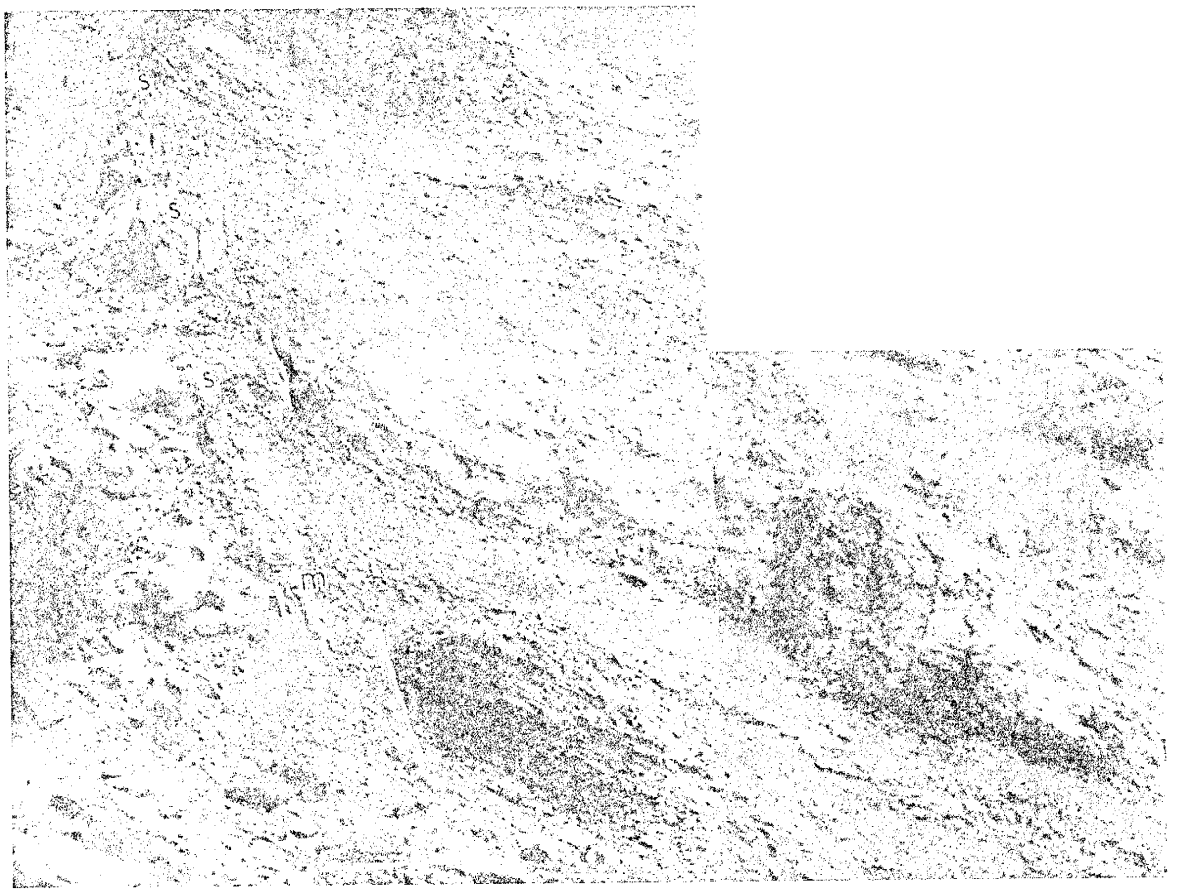

Figure 19. Photomosaic of sediments at the upper hanging wall bed at the Shooting Gallery site. Clay beds were dragged into contact with mixed zone (m, contact is dashed white line.) where they were rotated into parallelism with fault. Slip occurred along bedding planes forming a clay smear along the fault surface with small isolated pods of sand (s, outlined in white). The sand pods show similar geometries to fault-zone asperities that have been eroded by later faulting, described by Watterson et al. (1998).

bedded (~>1.5m) and consist of sands and/or gravels, beds are rotated and incorporated into the fault zone as relatively intact pods which contribute greatly to the fault-zone width. Also in some areas where the adjacent strata are clay rich or are thin (~<1.5m) alternating clay- and sand-rich beds, the beds are rotated into the fault plane with the clay-rich beds accommodating slip and being thinned (as evidenced by slickenside striae throughout the bed) with the sand beds are incorporated with out contributing much to the fault-zone width. It is important to note that these observations are preliminary and indicate only that flexural-slip folding may have occurred and be a factor in controlling fault-zone width and that future study is necessary to better constrain if flexural-slip folding is occurring and if so how it influenced fault-zone width.

Fault-zone width vs. displacement relationships

Previous workers have demonstrated that fault zone width may increase with displacement (see review by Hull, 1987). This issue is important when addressing the width differences for each unit in the Sand Hill fault zone since it is a growth fault. Different units in the hanging wall will have experienced increasing amounts of displacement with depth thus before effects of grain-size on fault-zone width can be addressed the effects of displacement on width need to be addressed. Plotting the thickness of the fault zone as it cuts different hanging wall units against their minimum displacement shows no relationship between fault-zone width and displacement (Fig. 20). The minimum displacements for the hanging wall units (with the exception of the displaced gravels at the Red Hill) are determined by the sum of the bed's exposed thickness plus the overlying beds.

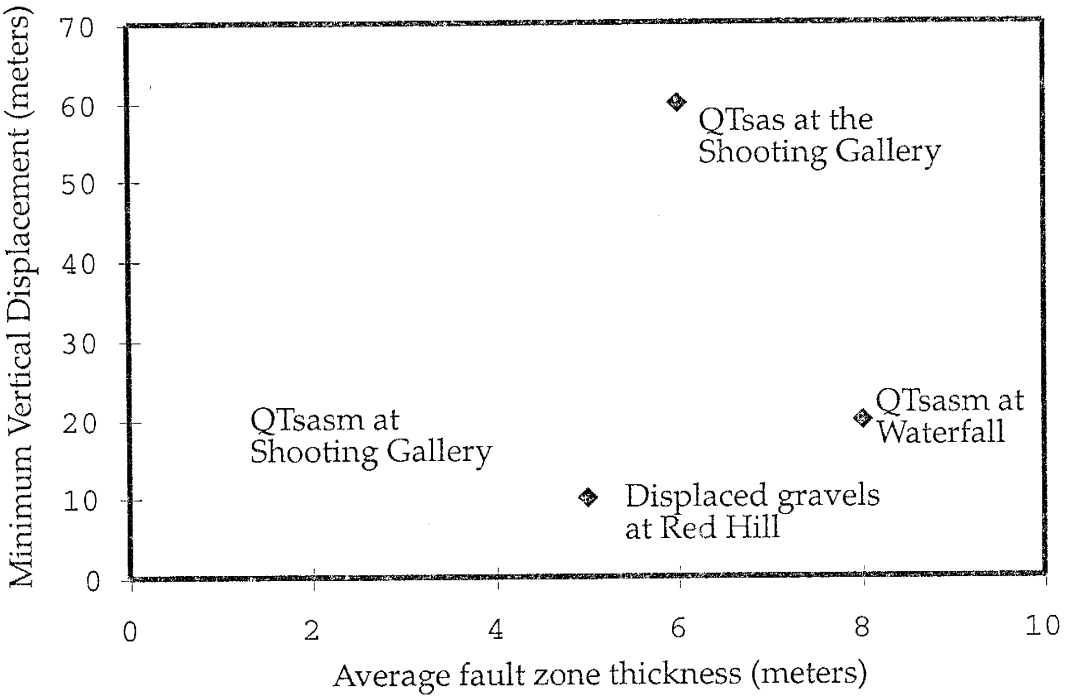

Figure 20. Plot of average fault-zone thickness vs. minimum vertical displacement. No apparent relationship is seen between displacement and thickness. Localities where data were gathered are indicated.

By examining figure 20 no apparent relationship is seen between displacement and fault-zone width. It is important to realize, though, that all these data are from the uppermost 60 meters of the hanging wall and a minor trend might be evident if the entire 600 meters of faulted hanging wall section were examined.

Fault-zone evolution

The observations present here suggest that it might be possible to predict the width of a fault zone in poorly consolidated sediments based upon the grain size distribution and bed thickness of the adjacent sediments. Where the fault zone cuts thickly bedded sand-rich sediment it should be wide and where it cuts clay-rich sediment or thinly bedded alternating sand and clay-rich beds it should be narrow. Also it should be noted that where the fault zone bends it would be wider as well due to increased structural complexities such as splays and bifurcations of the fault zone. The applicability of these relationships to faults other than the Sand Hill fault remains to be determined.

To better understand how the strain-hardening, strain-softening, and flexural-slip folding processes, discussed in previous sections, could work together to influence fault zone width and development a series of illustrations was created to show a hypothetical fault zone with various magnitudes of displacement (Fig. 21). To investigate how the variations in width of the Sand Hill fault formed it is important to consider these processes as a fault grows with increasing displacement.

Before discussing Figure 21 it is important to briefly discuss previous research regarding fault-zone growth, which describe structures similar to those

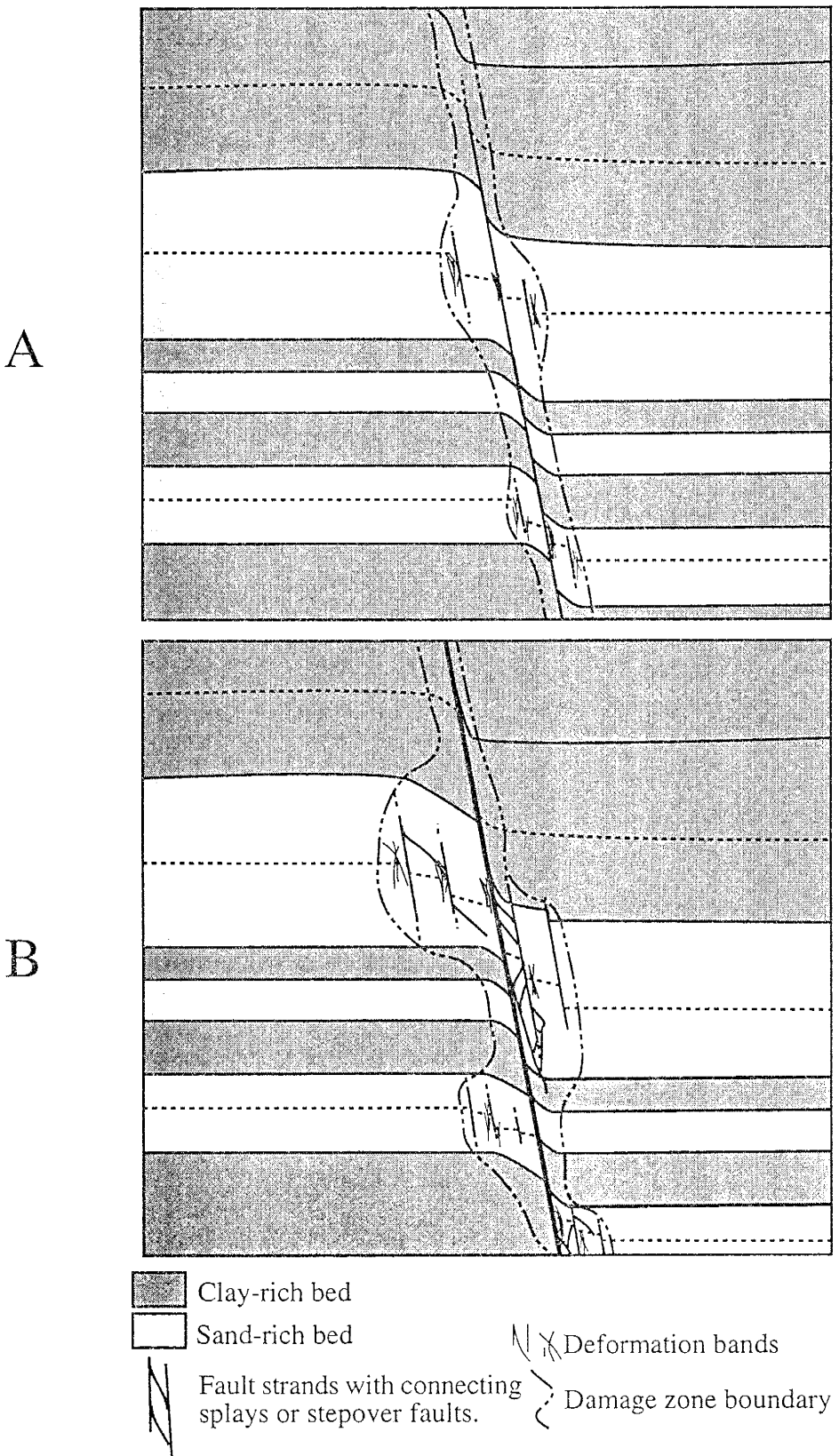

Figure 21. Model of fault zone evolution. Progression from 21A to 21B shown on this page; 21C and 21D shown on next page.

C

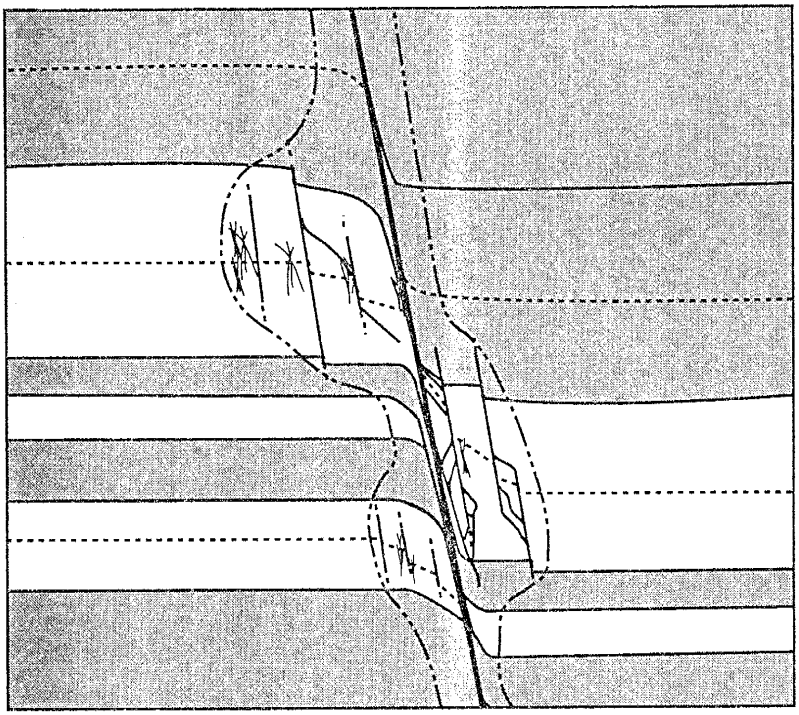

D

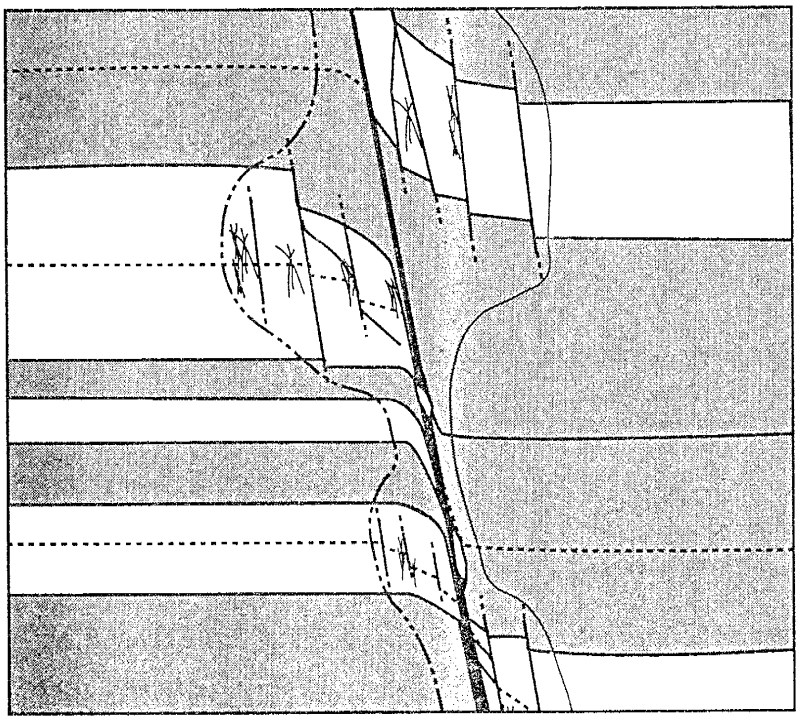

Figure 21 (continued).

observed in the Sand Hill fault. By comparing structures formed in other areas where the processes can be constrained to structures observed in the Sand Hill fault, it may be possible to gain a better understanding of the processes responsible for the variation in fault-zone width.

Numerous small faults may form during a single seismic event in a sand or sandstone bed (Aydin, 1978; Aydin and Reches, 1982; Aydin and Johnson, 1983). These faults may propagate into adjacent clay beds. During subsequent seismic events, strain hardening or softening can occur, causing individual faults to either widen or remain the same width. Where the initial faults are in a sand-rich unit, strain-hardening may occur. This may result in widening of the overall fault zone through the formation of additional deformation bands and /or slip surfaces. Also as faulting progresses, flexural-slip folding of the beds may occur at the fault tip (Cooke and Pollard, 1997). The folding of beds and resulting slip along bedding planes can contribute sediments to the fault zone. Where these sediments are sands they may behave more competently and be incorporated as pods of sediment isolated from their sources, as is commonly seen in the Sand Hill fault (Fig. 8, 14, 17). Where the incorporated sediment contains clay it was likely smeared and didn't add substantial thickness to the fault zone (Fig 16). Where the initial faults propagate into a clay-rich unit they may die out as the strain in the bed is accommodated by drag and smearing of the clay bed if it is less competent than the sand beds. Where a fault cuts the entire clay bed, strain softening is likely to occur. This will result in a fault zone whose width remains constant through reactivation. As displacement continues, the fault zone therefore is expected to widen where it cuts sand-rich units and remain constant in width where it cuts clay-rich units. At the contacts between clay- and sand-

rich beds, another process must occur to accommodate the differences in fault-zone width that result from differential growth of the fault zone in the different beds. From field observations of the Sand Hill fault, drag and smearing of the clay beds along slip surfaces, particularly adjacent to and within the core and mixed zones, appear to accommodate these differences.

The various stages of fault-zone development just described are illustrated in Figure 21 where a series of sand- and clay-rich beds are shown at various stages of faulting. The relationships depicted in this figure are based partly on interpretations of field relationships seen at the Sand Hill fault and partly on relationships between strain hardening, strain softening, and flexural-slip folding and the grain size and clay content of faulted sediments as previously discussed. If field observations at the Sand Hill fault are consistent with observations of other faults one might be able to compare processes responsible for the development of the observed structures.

In Figure 21A, small-displacement faults that initiated in the sand terminate in the adjacent clay beds. Displacement of the sand-rich beds was accommodated by several small faults and deformation bands whereas deformation of the clay-rich beds was accommodated by drag and slip along dragged bedding surfaces rotated into parallelism with the fault. Smearing of the clays against the slip surfaces is expected.

Figure 21B shows increased offset of beds along the faults. A throughgoing fault cut through both sand- and clay-rich beds. Within the thicker sand beds, where a clay-rich bed has not traveled past, the fault zone is wider as a result of the rotation and incorporation of sand beds, which are more competent than the clays, into the fault zone. The sands that were rotated into

the fault zone may have undergone strain hardening as evidenced by the zones of deformation bands that are adjacent to slip surfaces in the Sand Hill fault. Within the clay-rich beds there was increased drag, displacement by slip, and smearing along the slip surfaces. Several of the thinner clay-rich beds traveled past thin sand-rich beds resulting in a clay smear forming along the main slip surface at these locations. Where this occurred, strain hardening might have stopped in the sand beds because it would be easier for later events to reactivate the newly formed clay smear at the main slip surface. At this point it is important to realize that if a thicker bed had been rotated into the fault zone instead of a thin bed, more material would have been incorporated, resulting in a wider fault zone. If the material incorporated into the fault zone was sand rich it would behave more competently and make the fault zone wider than if it had been clay, which would be thinned with continued displacement.

Additional displacement was accompanied by preferential growth of the fault zone in the thicker sand-rich beds past which a clay bed has not traveled. For all other sand beds, the clay smear facilitated subsequent slip and the fault zone remained constant in width.

Figure 21D shows continued displacement with the fault zone width remaining relatively constant. This is because the displacement was sufficient enough so that a clay bed has traveled past all beds resulting in the formation of a continuous clay smear. This clay smear will localize deformation during later seismic events, allowing the fault zone to remain constant in width. Field relationships suggest that the fault-bounded blocks adjacent to the core will continue to rotate, to be extended, and to undergo mixing with increased displacement.

The thickness of clay-rich beds, the spacing between clay-rich beds, and the clay content of individual beds should influence the development of a clay smear in the fault core. Numerous models predicting smearing potential relative to bed thickness and spacing were reviewed by Yielding et al. (1997). Much variability exists between models, although the general principles used are similar. Typically the models assume that the clay smear or veneer will thin with increasing distance from its source, eventually becoming thin and patchy. The clay veneer at the Sand Hill fault does not appear to comply with the models summarized by Yielding et al. (1997). At the Sand Hill fault the clay veneer is continuous nearly everywhere with the exception of occasional gaps in the veneer that typically are <30cm long regardless of distance from nearest clay beds. This illustrates the need for further analysis and comparison of models to determine what relationships hold true and what mechanisms are responsible for the development of such a continuos clay veneer.

The spacing between clay-rich beds appears to have the greatest influence on fault-zone development along the Sand Hill fault (compare the bed spacing and fault zone thickness at the Shooting Gallery site with spacing and thickness at the Waterfall site). Where there are numerous thin, closely-spaced, clay- and sand-rich beds with a ratio $\simeq 1$, as in the Shooting Gallery, the displacement required to create a clay smear is relatively small and the fault zone should stop growing in width much earlier in its history. Where there are fewer and more widely spaced clay-rich beds, as in the Waterfall site, the displacement required to create a continuous clay smear is greater and the fault zone will continue to grow in width for a longer time, resulting in a wider fault zone.

Possible influence of the Sand Hill fault on Fluid Flow

To determine the possible influence of the Sand Hill fault on fluid flow two factors need to be established: 1), the relative permeabilities of structures, adjacent sediments, and sediments in the fault zone and 2), the spatial arrangement of the structures, adjacent sediments, and sediments incorporated into the fault zone. The relative permeabilities may be estimated by applying information gained from other studies. The spatial arrangement of the structures, adjacent sediments, and materials in the fault zone has been described in this study. The actual influence the Sand Hill fault has had on past fluid flow may be determined by examining elongate concretions. The location of fault zone cements relative to the regional groundwater flow gives insight into the possible influence that the fault has had and the locations of structures in the fault zone relative to adjacent sediments may help in modeling the fault zone in future studies.

The permeabilities of slip surfaces, deformation bands, and mixed zones developed in similarly poorly to unconsolidated sediment have been shown through air mini-permeameter and petrographic studies to be up to three orders of magnitude lower (not the mean) than adjacent sediment permeabilities, often with all porosity effectively occluded (Sigda et al., 1996; L.B. Goodwin and P.S. Mozley, written comm., 1997). Also the clay veneer that is present nearly everywhere in the fault zone is expected to have a very low permeability (Knipe, 1993, 1997; Gibson 1994). For future consideration of the actual influence the fault might have had on flow, the individual zones will be discussed below.

The damage zones have the least number of deformation bands and slip surfaces and are composed of sediment that is the same as the undeformed

sediment immediately adjacent to it. As a result this zone likely has the least influence on fluid flow.

The mixed zones have the greatest density of deformation bands and slip surfaces, and greatest amount of mixing (particularly grain-scale mixing). The mixed zones also have the most varied types of sediment within any given area. For instance, it is not uncommon to have the mixed zone composed of nearly all clay where the adjacent sediments are sands or the mixed zone can consist of sand and clay where the adjacent sediments are thick clay beds. For this reason the mixed zones may be the most important zones to address when making a model of how the fault has influenced fluid flow in the past. To model the mixed zones accurately, it would be necessary to determine what the controls are on their composition relative to the adjacent sediment, how each compositional element would influence flow, and what types of structures would be developed with each different compositional element found within the mixed zones.

The core zone may be expected to have a consistently low permeability since the clay veneer within it varies little in clay content, thickness, cementation, and structure throughout the fault zone. This clay veneer is analogous to clay smears that have been shown to act as effective barriers to fluid flow (Smith, 1980; Bouvier et al., 1989; Knipe et al., 1993; Gibson, 1994). The greatest variation in the core zone is the occurrence of gaps within the clay veneer which are rare and small (typically <30cm). To model the core one would need to determine a general permeability for it where the clay veneer is intact and where it is absent, and have a statistically valid technique for determining where the veneer is absent.

By examining cement distribution in regard to the regional flow pattern some relationships may be deduced. The majority of fault-zone cements occur in the hanging wall mixed zone where the hanging wall sediments are sands and/or gravels. The cements in the hanging wall mixed zone are best developed wherever the sediments in both footwall and hanging wall are sands or coarser sediments. Based on the orientations of oriented flow features outside of the fault zones and the location of the fault in regards to the Albuquerque Basin, it can be assumed that the regional groundwater flow was from the northwest to the southeast (Beckner, 1996). Knowing this, it appears that cross-fault flow must have occurred in order for the majority of cements to be precipitated on the hanging wall (basinward side) of the fault. This is reinforced by the presence of the best developed cements where sediments on both sides of the fault are coarse-grained (sands and coarser grained sediments). A pattern between degree of cementation and gaps in the core zone was not apparent, which may imply that the influence of the core zone may be nearly equal most everywhere. Finally, the orientation of flow features preserved in the fault zone, typically near the hanging wall mixed zone /damage zone boundary, are generally sub-vertical and sub-parallel to the fault zone (Fig. 4). This implies that at the time of their formation flow was reoriented to a generally fault-parallel orientation.

Timing of cementation

Fault-zone cementation is interpreted to have occurred at least during and after the majority of faulting occurred. Slickenside striae are commonly seen on cemented surfaces. Since the cemented surfaces must have been present prior to the formation of the slickenside striae within them, it follows that they formed

before the last faulting event. Since the cemented surfaces are oriented parallel to slip surfaces and deformation bands, it is unlikely that they were present prior to faulting. This is especially true where these features are cemented themselves. Furthermore the majority of the fault-zone cements are concentrated within the hanging wall mixed zone indicating that enough displacement must have occurred to form the mixed zones prior to cementation. Since the most-extensively cemented zones correspond with areas where not only the hanging wall sediments are coarse grained but also the footwall sediments are coarse, it follows that some cementation occurred after the current juxtaposition of units occurred.

Conclusions and implications

The primary conclusion of this thesis is that fault-zone width is dependent on the thickness, spacing, and clay content of sediments adjacent to the fault. Where the adjacent sediments are ~$\geq$ 82% sand and are thickly bedded, the fault is typically wide (>2 m). Where the adjacent sediments ~< 82% sand or are thinly bedded alternating beds of clay and sand, the fault is typically narrow (<2m). The processes responsible for widening of the fault zone may be strain hardening, as evidenced by a series of closely spaced structures, and flexural slip folding, as evidenced by rotation of beds into the fault plane with slickenside striae preserved on their bedding planes. Strain softening is one process which may be responsible for allowing the fault to remain narrow where it cuts clay-rich (~<82% sand) units as evidenced by the presence of significantly fewer structures present in clay units.

This has important implications because it may allow qualitative prediction of fault-zone architecture where the sediments on both sides of the fault are known by subsurface methods. This is especially useful if these relationships can be extrapolated to other faults in similar settings. If after further investigation it is shown that similar processes are active in faults cutting similar materials then it may be possible to predict their fault-zone architecture at depth if the grain-size and clay content and bed thickness and spacing of adjacent strata can be constrained.

References

Anderson, L.J., Osborne, R.H., and Palmer, D.F., 1983, Cataclastic rocks of the San Gabriel fault - An expression of deformation at deeper crustal levels in the San Andreas fault zones: Tectonophysics, v. 98, p. 209-251.

Anderson, T.W., Welder, G.E., Lesser, G., and Trujillo, A., 1988, Region 7, central alluvial basins, in Back, W., Rosenshein, J.S., and Seaber, P.R., eds., The Geology of North America, v. 0-2, Hydrogeology: Boulder, Colorado, Geological society of America, p. 81-86.

Antonellini, M. and A. Aydin, 1994, Effect of faulting on fluid flow in porous sandstones: petrophysical properties: AAPG Bulletin, v. 78, p. 355-377.

Antonellini, M. and A. Aydin, 1995, Effect of faulting on fluid flow in porous sandstones: geometry and spatial distribution: AAPG Bulletin, v.79, p. 642-671.

Aydin, A., 1978, Small faults formed as zones of deformation bands and as slip surfaces in sandstone: Pure and Applied Geophysics, 16, 931-942.

Aydin, A. and Johnson, A.M., 1978, Development of faults as zones of deformation bands and as slip surfaces in sandstone: Pure and applied geophysics, v. 116, p. 913-930.

Aydin, A. and Johnson, A.M., 1983, Analysis of faulting in porous sandstones: Journal of Structural Geology, 5, no.1, 19-31.

Aydin, A. and Reches, Z., 1982, The number and orientation of fault sets in the field and in experiments: Geology, v. 10, p. 107-112.

Barnett, J.A.M., Mortimer, J., Rippon, J., Walsh, J.J., and Watterson, J., 1987, Displacement geometry in the volume containing a single normal fault, AAPG Bulletin, v. 71, p. 925-937.

Beckner, J.R., 1996, Cementation processes and sand petrography of the Zia Formation, Albuquerque Basin, New Mexico, [M.S. thesis]: New Mexico Tech, Socorro, NM, 146p.

Bouvier, J.D., Kaars-Sijpesteijn, C. H., Kluesner, D.F., Onyejekwe, C.C., and van der Pal, R.C., 1989, Three-dimensional seismic interpretation and fault sealing investigations, Nun River field, Nigeria: AAPG Bulletin, 73, 1397-1414.

Borg, I., Friedman, M., Handin, J., and Higgs, D.V., 1960, Experimental deformation of St. Peter Sand: a study of cataclastic flow, *in* Griggs, D. and Handin, J., eds., Rock deformation: Geological Society of America Memoir 79, p. 133-191.

Bruhn, R. L., Parry, W.T., Yonkee, W.A., and Thompson, T., 1994, Fracturing and hydrothermal alteration in normal fault zones: Pure and Applied Geophysics, v. 142, p. 139-157.

Byerlee, J.D., 1993, Model for episodic flow of high-pressure water in fault zones before earthquakes: Geology, v. 21, p. 303-306.

Caine, J.S., Evans, J.P., Forster, C.B., 1996, Fault-zone architecture and permeability structure: Geology, v.24, p. 1023-1028.

Cather, S.M., 1997, Toward a hydrogeologic classification of map units in the Santa Fe Group, Rio Grande rift, New Mexico: New Mexico Geology, v. 19, p. 15-21.

Cather, S.M., Connell, S.D., Heynekamp, M.R., and Goodwin, L.B., 1997, Map of the Sky Village SE 7.5-minute quadrangle, Sandoval county, New Mexico: New Mexico Bureau of Mines and Mineral Resources Open-file report, DGM 9.

Chester, F. M., and Logan, J.M., 1986, Implications for mechanical properties of brittle faults from observations of the Punchbowl fault zone, California: Pure and Applied Geophysics, v. 124, p. 77-106.

Cooke, M.L. and Pollard, D. D., 1997, Bedding-plane slip in initial stages of fault-related folding, Journal of Structural Geology, Vol. 19, p. 567-581.

Donath, F.A., and Parker, R. B., 1964, Folds and faulting, Geological Society of America Bulletin, v. 75, p. 45-62

Foxford, K.A., Garden, I.R., Guscott, S.C., Burley, S.D., Lewis, J.J.M, Walsh, J.J., Watterson, J., *in press* , The field geology of the Moab Fault, In *Huffman, C., Doelling, H.H. and Willis, G., (eds.) Geology and Resources of the Paradox Basin.*

Fowles, J. and Burley, S.D., 1994, Textural and permeability characteristics of faulted, high porosity sandstones: Marine and Petroleum Geology, v. 11, p. 608-623.

Frydman, S., 1976, The strain hardening behavior of particulate media: Canadian Geotechnical Journal, v. 13, p. 311-323.

Gibson, R.G.,1994, Fault-zone seals in siliclastic strata of the Columbus Basin, offshore Trinidad, AAPG Bulletin 78, p. 1372-1385.

Goodwin, L.B. and Haneberg, W.C., 1996, Deformational fabrics and inferred permeability of faulted sands from the Rio Grande rift, New Mexico: Geological Society of America Abstracts with programs, v. 28, p. A-255.

Hawley, J.W., and Haase, C.S., 1992, Hydrogeological framework of the northern Albuquerque Basin: New Mexico Bureau of Mines and Mineral Resources Open File Report 387, 147 p.

Hawley, J.W., Haase, C.S., and Lozinsky, R.P., 1995, An underground view of the Albuquerque Basin, *in* Proceedings of the 39th Annual Water Conference: Las Cruces, New Mexico Water Resources Research Institute.

Hull, J., 1988, Thickness-displacement relationships for deformation zones: Journal of Structural Geology, v. 10, p. 431-435.

Jameson, W.R., and Stearns, D.W., 1982, Tectonic deformation of Wingate Sandstone, Colorado National Monument: Bulletin of the American Association of Petroleum Geologists, v. 66, p. 2584-2606.

Kelley, V.C., 1977 Geology of the Albuquerque Basin, New Mexico: New Mexico Bureau of Mines and Mineral Resources Memoir 33, 59p.

Knipe, R. J., 1993, The influence of fault zone processes and diagenesis on fluid flow, *in* A. D. Horbury and A. G. Robinson, eds., Diagenesis and Basin Development, American Association of Petroleum Geologists, Studies in Geology #36, p. 135-148.

Knipe, R. J., 1997, Juxtaposition and seal diagrams to help analyze fault seals in reservoirs: AAPG Bulletin, v. 81, n. 2, p. 187-195.

Machette, M.N., 1978, Geologic map of the San Acacia quadrangle, Socorro County, New Mexico: USGS, Geologic Quadrangle Map GQ-1415, scale 1:24,000.

Maltmann, A., 1987, Shear zones in argillaceous sediments-an experimental study *in* Jones, M.E. and Preston, R.M.F., editors, Deformation of sediments and sedimentary rocks, London Geological Society Special Publication no. 29, p. 77-90.

Marone, C., Raleigh, C.B., and Scholz, S.H., 1990, Frictional behavior and constitutive modeling of simulated fault gouge: Journal of Geophysical Research, v. 95, p. 7007-7025.

Mifflin, M.D., 1988, Region 5, great basin, *in* Back, W., Rosenheim, J.S., and Seaber, P.R., eds., The geology of North America (volume 0-2), Hydrogeology: Boulder, Colorado, Geological Society of America, p. 69-78.

Morrow, C.A., Shi, L.Q., and Byerlee, J.D., 1982, Strain hardening and strength of clay-rich fault gouges: Journal of Geophysical Research, v. 87, no. B8, p. 6771-6780.

Mozley, P.S. and Goodwin, L.B., 1995, Patterns of cementation along a Cenozoic normal fault: A record of paleoflow orientations, Geology, v. 23, p. 539-542.

Mozley, P.S., and Davis, J.M.D., 1996, Relationship between oriented calcite concretions and permeability correlation structure in an alluvial aquifer, Sierra Ladrones Formation, New Mexico: Journal of Sedimentary Research, v. A66, p. 11-16.

Pittman, E. D., 1981, Effect of fault-related granulation on porosity and permeability of quartz sandstones, Simpson Group (Ordovician), Oklahoma, AAPG Bulletin 65, 2381-2387.

Rudnicki, J.W., 1977, The inception of faulting in a rock mass with a weakened zone: Journal of Geophysics Research, v. 82, p. 844-854.

Sibson, R.H., 1977, Fault rocks and fault mechanisms: Geologic Society of London Journal, v. 133, p. 191-231

Sigda, J.M., Mozley, P.S., Goodwin, L.B., and Haneberg, W.C., 1996, Small displacement fault controls on single phase permeability in poorly consolidated sands, Santa Fe Group, New Mexico [abstract]: GSA 1996 Annual Meeting Abstracts with Programs.

Skempton, A.W., 1942, "An Investigation of the Bearing Capacity of a Soft Clay Soil," J. Inst. Civil Engrs., vol. 18, p.307.

Smith, D.A., 1980, Sealing and nonsealing faults in Louisiana Gulf Coast Salt Basin, AAPG Bulletin, 64, 145-172.

Smith, L., Forster, C.B., and Evans, J.P., 1990, Interaction of fault zones, fluid flow, and heat transfer at the basin scale, *in* Hydrogeology of permeability environments: International Association of Hydrogeologists, v. 2, p.41-67.

Tedford, R. H., 1982, Neogene stratigraphy of the northwestern Albuquerque Basin: New Mexico Geological Society Guidebook 33, p. 271-278.

Underhill, J.R., and Woodcock, N.H., 1987, Faulting mechanisms in high porosity sandstones; New Red Sandstone, Arran, Scotland, *in* Jones, M.E. and Preston, R.M.F., *eds.*, Deformation of sediments and sedimentary rocks: Geological Society of London Special Publication, v. 29, p. 91-105.

Watterson, J., Childs, C., and Walsh, J.J., 1998, Widening of fault zones by erosion of asperities formed by bed-parallel slip, Geology, v. 26, p. 71-74.

Wright, H.E., 1946, Tertiary and Quaternary geology of the lower Rio Puerco area, New Mexico: Geological Society of America Bulletin 57, 383-456.

Yielding, G., Freeman, B., and Needham, D.T., 1997, Quantitative fault seal prediction: AAPG Bulletin, v.81, p. 897-917.

Appendix A: Description of Photomosaics of the Sand Hill Fault Zone

Authors:
Michiel Heynekamp
B. Christopher Dimeo

Introduction

Four photomosaics were constructed to illustrate the variability of structures and sediments within the core and mixed zones of the Sand Hill fault zone. The first photomosaic, from the Shooting Gallery site, was selected to represent the narrow and relatively structurally simple end member of the mixed zone. The second and third are of the Waterfall site, where the mixed zone is relatively structurally complex and wide. The fourth, from the Shooting Gallery site, illustrates an area where the core is relatively sand-rich in comparison with the more typical clay-rich core zone.

The degree of deformation within the mixed zone ranges from slivers or pods of minimally deformed beds to sediments whose original bedding and sedimentary textures have been completely destroyed through grain-scale mixing. The mixed zone has therefore been divided into three units according to degree of tectonic mixing: M1 = minimally deformed beds, which exhibit varying degrees of rotation in the fault zone; M2 = deformed beds that have undergone considerable extension and thinning, often resulting in a fault-parallel foliation; and M3 = sediments that have undergone grain-scale mixing, resulting in homogenization of original textures and compositions.

Photomosaic #1

Photomosaic #1 consists of 7 mosaics, each of which represents one terrace (the outcrop was terraced to enhance exposure). The fault-zone units are traced across the different terraces. A mosaic of the entire outcrop illustrates the spatial relationship between the individual terrace mosaics.

The mixed zone in this area is dominantly composed of M1 and M2 units. Across the damage zone - mixed zone boundary, bed "A" is vertically displaced ~8 m. The sediments in M1 are mainly little deformed sands. Bedding is rotated, extended, and thinned slightly. M2 is composed of fault-parallel clay-rich beds. The sediments are foliated and dissected by numerous slip surfaces. M3 units generally border the core zone, are composed of minor amounts of sand supported in a clay matrix, and are typically foliated.

The core zone is largely composed of a ~ 20 cm wide, clay-rich veneer. The clay veneer is continuous except where it is transected by short, ~ 10 -15 cm long pods of foliated sand. The clay veneer exhibits a foliation defined by the alignment of clays.

The damage zone is poorly exposed. Where exposed, it has minimally dragged sediments that are dissected by numerous deformation bands.

The results of petrographic work summarized in the main report suggest that M2 and M3 units at this site will have very low, shale-like permeabilities.

Photomosaic #2

Photomosaic #2 includes two detailed mosaics. The first traverses the fault zone; the second follows the widest strand of the core zone. Two outcrop-scale mosaics show the locations of the detailed mosaics.

The mixed zone is cut by numerous small-displacement (<1m) slip surfaces and exhibits a fault-parallel foliation defined by compositional banding. M1 is present near the mixed zone - damage zone boundary and consists of dragged sands from adjacent beds. It is dissected by numerous deformation bands and small-displacement slip surfaces. Photomicrographs of the sands from this area (sample SHFNN81) are presented in Figs. 10 and 11 of the main report. The mixed zone is dominantly composed of M2 and M3 units. M2 units are largely sandy, but contain discontinuous lenses and irregular bodies of clay and gravel. M3 units are generally clay-rich and contain minor amounts of sand in a clay matrix. Petrographic work indicates that M3 units, clay-rich portions of M2, and deformation bands and slip surfaces in sands with plentiful volcanic clasts should all have shale-like permeabilities.

The core zone is generally composed of a well foliated clay veneer and minor amounts of foliated sand. It bifurcates into multiple strands at this outcrop. The strands are linked by numerous slip surfaces, which are difficult to trace throughout the fault zone. Sand is locally a minor constituent of the clay veneer, with sand grains and clusters of grains suspended in a clay matrix.

The damage zone is dissected by numerous small-displacement slip surfaces and deformation bands. Beds are dragged near the boundary with the mixed zone.

Photomosaic #3

Photomosaic #3 was taken from an area approximately 5 meters south of photomosaic #2. It illustrates the footwall mixed zone and the core zone.

The mixed zone is largely composed of M1 and M2 units. The majority of M1 is poorly exposed; where exposed it consists of sand-rich beds that have been displaced and dragged several meters. M2 mostly includes extended and thinned sand-rich beds dissected by numerous small-displacement slip surfaces. M3 generally contains foliated clay-rich sediments. Minor amounts of sand are supported in the clay matrix. The M3 zones are generally adjacent to core zone strands. Photomicrographs of samples SHFNS10 and SHFNS2x are shown in Figs. 13 and 12 of the main report, respectively.

The core zone bifurcates into multiple strands from the top to the bottom of the outcrop. It generally includes a foliated clay veneer, continuous except where it is transected by ~10-15cm long sand-rich, foliated bodies. Volcanic ashes similar to those in adjacent beds are also common within the core zone. The ash layers are composed mainly of clay-sized material which is generally altered to clay minerals.

Photomosaic #4

Photomosaic #4 is representative of areas along the fault where the clay veneer is poorly developed. The core is composed of foliated sand ribbons, which may be preferentially cemented, interlayered with thin, locally discontinuous clay veneers. The clay veneers are poorly developed and contain a large proportion of sand. Petrographic study of sandy clay, discussed in the main report, suggests that these sandy veneers will have very low permeabilities.

Appendix B: Sample collection and grain-size analysis

Sample collection

To ensure that samples taken for grain-size analysis were representative of the areas sampled, several different methods were employed depending on the unit sampled. Samples for grain-size analysis were taken from bedding adjacent to the fault zone, from the mixed zones, and from the core zone. Sample sites are indicated on the map and/or cross-sections.

The surface of the outcrop was excavated to sample bedding. Excavation of the outcrop is important in order to ensure that sampling was of the desired unit and not colluvium. This excavation was done one of two ways depending on bed thickness. If the bed was several meters thick, excavation was done at several locations across the bed at approximately .5 m spacing. A sample of about 50 grams was taken from each excavation site. All samples from the bed were placed in the same sample bag. If the bed's thickness was less than about 1.5 meters, the entire bed was exposed through excavation. From this exposure several 50 gram samples were taken to fully represent bed-scale grain size variations. Once again all samples were placed together.

For mixed zone samples, a traverse across the mixed zone was excavated from which several samples were taken. The samples were only taken from sediments that had been tectonically mixed and not from intact pods. Because there can be great variability in the grain-size of the mixed zone, each feature (i.e. sand ribbon, clay veneer, etc.) was sampled. The sample size taken for each feature depended on its relative volumetric proportion to other features within

the mixed zone to ensure that the overall sample represented the variation present within the entire mixed zone at that point location.

A sample was taken of all material present within the core zone at a given sample location. Typically the core zone is .1 -.2 meters wide and a section spanning completely the entire zone could be removed by hand. If the core zone was wider, a sample of each element present would be taken in proportion to its relative amount present in outcrop.

Once the samples were collected they were disaggregated by hand and processed through a splitter until the sample size was ~ 100 grams. The samples were further split according to their general grain sizes. Clay-rich samples were split until they were ~20 grams. Sand-rich samples were split until they were ~40 grams. Once the samples were split their grain-size distribution was determined using wet-sieving and settling time techniques.

Grain-size analysis

The particle size analysis procedure used was modified from Day (1965) and Jackson (1969) as described in University of New Mexico's Soil laboratory analyses handbook.

Equipment:

Analytical Balance
125 ml Erlenmeyer flasks
50 ml graduated cylinder or pipette
No. 5 stoppers
Shaker table
Water bottle (deionized)
63μm Sieve
Funnel
1200ml fleakers and caps
Marble platform
Pipette (20 or 15 ml)
Aluminum sample dishes

Reagents
Dispersing agent: 10% Sodium Pyrophosphate

Procedure:

1. If sample contains abundant organic matter or carbonate it must be removed through acid digestion.
2. Weigh 125 ml Erlenmeyer flask to the nearest .01g. Weigh out and record ~20 grams of the fine fraction (<2 mm) and place in the Erlenmeyer flasks. Use 40 grams of sample if texture is sandy or sandy loam, and 10 to 15 grams for clays.
3. The weight of the dispersant must be known. Prepare a blank using a 125 ml Erlenmeyer flask (30ml of deionized H_20 +50 ml of Sodium Pyrophosphate). Treat this the same as the rest of the samples for the following procedure.
4. Pipette 50ml of the dispersant solution into a flask with sample. Add approximately 30 ml deionized H_20 to flask. Place flask on a mechanical shaker table. Shake for a minimum of four hours in order to disperse the clays. For clay-rich samples 12 hours is recommended.
5. Wet sieve the clay and silt fraction using a 63μm sieve into 1200ml fleakers. Fill fleakers to 1200ml mark but do not overfill. Wash the sand left in the sieve back into the Erlenmeyer flask. Oven dry the sample. Weigh and record the sand fraction when dry. Pour solution from blank into fleaker and fill to 1200 ml.
6. Cap fleakers and shake each vigorously for ~30 seconds at 2 minute intervals and record the time. Note the room temperature.

7. Wait the required duration of time according to table 1 to allow the materials greater than 2μm to settle below the 10cm depth. In the meantime weigh, record, and label aluminum sample dishes to the nearest .0001 gram.
8. At the appropriate time extract a 20 ml or 25 ml aliquot of clay suspension using a pipette. Collect the sample at the 10 cm depth. Empty pipette into appropriate aluminum clay sample dish. Oven dry clay sample dish at 105 °C for 8 hours. Allow the dish to cool in a dessicator before weighing the sample.
9. Enter data into the data sheet (Fig. 19) and perform calculations.

Table 1: Settling time for 10 cm fall of a 2μ (Clay) particle.

Temperature C°	hour	min
5	12	5
6	11	45
7	11	20
8	11	00
9	10	45
10	10	25
11	10	10
12	9	50
13	9	35
14	9	20
15	9	05
16	8	50
17	8	35
18	8	25
19	8	10
20	8	00
21	7	50
22	7	40
23	7	25
24	7	15
25	7	05
26	6	55
27	6	45
28	6	40
29	6	30
30	6	25

This thesis is accepted on behalf of the faculty

of the institute by the following committee:

Advisor

April 30, 1998

Date